ST. ANTHONY FALLS HYDRAULIC LABORATORY
UNIVERSITY OF MINNESOTA

Project Report No. 25

EXPERIMENTAL DESIGN STUDIES ON FREE-JET WATER TUNNELS

Submitted by
LORENZ G. STRAUB
Director

Prepared by
CHARLES D. CHRISTOPHERSON

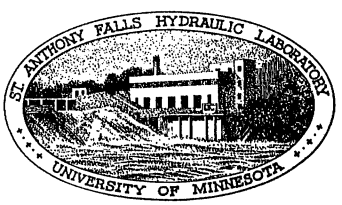

September, 1951

Prepared for
OFFICE OF NAVAL RESEARCH
Department of the Navy
Washington, D.C.

Under Office of Naval Research Contract N8onr-66202

PREFACE

The following Technical Report is based on the design study of free-jet water tunnels carried out at the St. Anthony Falls Hydraulic Laboratory of the University of Minnesota and sponsored by the Office of Naval Research, Department of the Navy, under Contract N8onr-66202, Research and Development Board No. NR-062-065.

The study was made and the report written by Charles D. Christopherson under the general supervision of Dr. Lorenz G. Straub, Director of the St. Anthony Falls Hydraulic Laboratory. The discussion of open-jet and closed-jet water tunnels was based on an unpublished analysis by James S. Holdhusen. The experimental studies embody numerous suggestions contributed by Professor John F. Ripken, who also critically reviewed the report. John J. Casey assisted in the experimental work and preparation of illustrations, and Leona S. Wray assisted in preparation of the manuscript.

A B S T R A C T

A study of the design and operating characteristics of free-jet water tunnels is presented. Included is a brief analysis indicating that this type of water tunnel is particularly well suited for the empirical analysis of steady-state cavities which form about solid bodies moving through water at extremely low cavitation indices. It is pointed out that the conventional closed-jet and open-jet types possess inherent limitations on the quality of the test-section flow and the accuracy and applicability of the measurable flow properties at these low cavitation indices.

The experimental apparatus is described verbally and photographically. It was designed for the production and study of a test jet of circular cross section having a 2-in. diameter and an effective length of 6 diameters. The jet could be directed vertically upward, vertically downward, and horizontally. Facilities for the production and analysis of steady-state cavities within the jet are also described.

The experimental studies and the results are discussed. Included are observations concerning air entrainment by the jet, visual qualities of the jet, total head Pitot tube traverses of the jet, and steady-state cavities within the jet at cavitation indices as low as 0.015. The report concludes with general recommendations concerning the design of free-jet water tunnels.

C O N T E N T S

LIST OF ILLUSTRATIONS

GLOSSARY

A = the cross-sectional area of the test-section flow.

A_m = the maximum cross-sectional area of a steady-state cavitation bubble.

B = $(D/2)/(U_o^2/2g)$.

D = the diameter of a free jet of circular cross section.

D_o = the test-section depth of a horizontal test section; the diameter of a cylindrical test section of circular cross section; the diameter of a circular free jet at the upstream end of the test section; the diameter of a contraction of circular cross section at its downstream face.

d_m = the maximum diameter of a steady-state cavitation bubble or of a non-cavitating body of circular cross section.

d = diametrical distance.

e = a subscript referring to a plane through the downstream end of the test section.

F = the drag force on the test section and a cavitation body supported within the test section.

Fr = the Froude number = U_o^2/gL.

f = a shape factor depending on the shape of a cavitating body such that $0.9 \leq f \leq 1.0$ and $f \to 1$ as $\sigma_k \to 0$.

K_1 = the head drop due to energy loss in the test section divided by $U_o^2/2g$.

K_2 = the maximum head drop in the transition region from the test section to the diffuser of a conventional water tunnel due to curvilinear flow in this region, also divided by $U_o^2/2g$.

L = the axial distance downstream from the downstream face of the contraction.

ℓ = the axial length of a steady-state cavitation bubble.

o = a subscript referring to a plane through the upstream end of the test section.

p = the absolute static pressure.

p_c = p which is characteristic of a particular cavitation phenomenon.

p_{cr} = p at a point when cavitation is incipient at the point.

p_e = p on the centerline of the test section at the downstream face.

p_k = p within a steady-state cavity.

p_o = p on the centerline of the test section at the upstream face.

p_t = p at the top of the plane of minimum flow cross section in the test section of a conventional water tunnel.

p_v = the vapor pressure of a liquid with reference to absolute zero.

r = radial distance from the contraction axis.

t = photographic exposure time.

U = the speed of a point in a liquid relative to a point fixed in a solid body.

U_c = U on the centerline of the jet, relative to the test section, at an axial distance L downstream of the downstream face of the contraction.

U_o = U on the centerline of the test section at the upstream face relative to a cavitation head within the test section.

U_t = U at the top of the plane of minimum flow cross section in the test section of a conventional water tunnel relative to the test section.

x = the axial distance downstream from the upstream face of the contraction.

y = the distance below the contraction axis of the centerline of a horizontal free jet.

ρ = the mass density of a liquid.

σ = the cavitation index.

σ_{cr} = σ referred to incipient cavitation.

σ_{cr_b} = σ on the centerline of the test section at the upstream end when cavitation first occurs at both the transition from the test section to the diffuser and the top of the plane of minimum flow cross section of a conventional water tunnel.

σ_{cr_d} = σ on the centerline of the test section at the upstream end when cavitation first occurs at the transition from the test section to the diffuser of a conventional water tunnel.

σ_{cr_t} = σ on the centerline of the test section at the upstream end when cavitation first occurs at the top of the plane of minimum flow cross section in the test section of a conventional water tunnel.

σ_k = σ referred to steady-state cavitation.

EXPERIMENTAL DESIGN STUDIES ON FREE-JET WATER TUNNELS

I. INTRODUCTION

A free-jet water tunnel is one of the four types of variable pressure water tunnels characterized by basic test-section design (the other three are the open-jet, the closed-jet, and the free-surface). The purpose of this study was to develop a knowledge of the characteristics of this type of water tunnel, which would add emphasis to its feasibility as an experimental tool and subsequently act as an aid to the designer of such a tool. To implement the study, a small free-jet water tunnel was constructed having a 2-in. jet diameter and an effective test-section length of 6 jet diameters. This apparatus will be more completely described later in this paper; however, it should be noted that this initial design was of a very general nature and there was no intent that it serve as a geometrical model for a larger system.

Studies were made with the test jet oriented in three directions--vertically upward, vertically downward, and horizontally. As would be expected from the nature of the study, most of the results and conclusions obtained do not lend themselves well to an all-inclusive, itemized summary; they are, therefore, to be found scattered throughout the following pages and summarized in only a very general nature in the last section. The following section will be concerned with a brief, approximate analysis which indicates the need for the free-jet type of water tunnel if certain investigations are to be carried out, and it points out some of the operational problems inherent in such a system. The remainder of the paper deals with the experimental apparatus, procedure, and results of this study. Symbols are defined in a glossary and where first used and comply in so far as possible with standard practices. Where reference is made to "conventional water tunnels" the open-jet and closed-jet types are implied. A list of the illustrations used can be found in the forepart of this publication, and the references, indicated by numbers enclosed in brackets, are listed on the last page.

II. SIGNIFICANT CHARACTERISTICS OF FREE-JET WATER TUNNELS

In studying the relative motion between incompressible fluids and solid bodies submerged within these fluids such that there are no free surface effects, use has long been made of open-jet and closed-jet variable-pressure

water tunnels; however, the free-jet water tunnel is a rather recent innovation developed by H. Reichardt [1]. The purpose of any water tunnel is to create certain predetermined flow conditions, and a measure of the efficiency of the water tunnel is the extent to which the desired flow conditions are simulated by the water tunnel flow and the availability of this flow for experimental analysis. Each type has certain advantages and disadvantages with respect to the others, and, by the nature of these, each is preferable for certain types of investigations, e.g., the open-jet water tunnel is particularly well adapted to the study of the flow phenomena associated with propellers. With this in view, the intent in this section is to establish that the free-jet water tunnel is the type best suited for studying steady-state cavitation bubbles which form about solid bodies under extreme cavitation conditions. The superiority of the free-jet water tunnel for this type of study stems from two basic factors: (1) the necessary flow conditions can best be produced in a free-jet water tunnel; and (2) the cavitation index representative of these flow conditions can be accurately determined in a free-jet water tunnel but cannot for a closed-jet or open-jet water tunnel.

Considering first the cavitation index, it is commonly defined at a point in a flowing liquid as follows:

$$\sigma = \frac{p - p_c}{\rho \frac{U^2}{2}}$$

where σ = the cavitation index,

U = the speed of the point in the liquid relative to a point fixed in a solid body.

ρ = the mass density of the liquid,

p = the absolute static pressure (at the point), and

p_c = the absolute static pressure which is characteristic of the particular cavitation phenomenon of interest.

The term p_c is the weak point in the definition. If the cavitation index is to be applied to the study of incipient cavitation, then the value of p_c should be taken as that at which cavitation first begins; however, if the cavitation index is to be applied to the study of steady-state cavities, then p_c should be taken as the actual pressure within a steady-state cavity in the liquid. In the former case and in the latter case when the steady-state cavities are natural cavities resulting from reduced pressures in a region, p_c is approximately

equal to the vapor pressure, p_v, at the temperature of the liquid at the point in question. However, in any given practical flow problem it is more likely than not to be true that the static pressure at which cavitation begins, the static pressure within a steady-state cavitation bubble which is vapor filled, and the vapor pressure of the flowing liquid will be three different numerical quantities. In order to differentiate between the cavitation index as applied to the study of steady-state cavitation bubbles and the study of incipient cavitation, let σ_k apply to the former case and σ_{cr} apply to the latter, such that

$$\sigma_k = \frac{p - p_k}{\rho \frac{U^2}{2}}$$

$$\sigma_{cr} = \frac{p - p_{cr}}{\rho \frac{U^2}{2}}$$

where p_k = the absolute static pressure within a steady-state cavity, and
p_{cr} = the absolute static pressure at a point when cavitation is incipient at the point.

It is considered throughout the remainder of this paper that the situation of interest in the study of steady-state cavities is that in which a cavity has formed behind a solid body (cavitation head) placed in a region in which the static pressure and velocity were initially uniform throughout; this region consists of the test section in the case of water tunnel studies. If σ_k is defined within the cavity, then $p = p_k$ and $\sigma_k = 0$ for all steady-state cavities; hence if the cavitation index is to be used as a modeling parameter, it must be so defined that $\underline{p}$ is not taken within the cavity and such that σ_k is descriptive of the particular steady-state cavity under study and is equal to zero only for a special case. To accomplish this it is conventional to define σ_k in one of the two following manners: (1) the value of σ_k is evaluated at a point in the uniform flow region such that the flow at the point is not affected by the existence of the cavitation head and cavity at another point; (2) the value of σ_k is evaluated at a point in a flow from which the cavitation head has been removed which would lie within the cavitation head or its cavity if it were present. Under the ideal conditions of uniform pressure and velocity in the undisturbed flow region, the two definitions would result

in the same numerical value of σ_k for a given study. In the practical case of water tunnel testing, the former definition has the advantage of permitting the evaluation of σ_k at the same time that the steady-state cavity being studied exists in the test-section flow; hence it is the one adopted for use in the remainder of this paper. To be more specific, let σ_k be the cavitation index on the centerline at the upstream face of the test section such that

$$\sigma_k = \frac{p_o - p_k}{\rho \frac{U_o^2}{2}}$$

where p_o = the absolute static pressure at this point, and
U_o = relative speed between the cavitation head and liquid at this point.

Now consider the components p_o, p_k, and $\rho(U_o^2/2)$ separately as regards their evaluation and the accuracy and effectiveness of σ_k as just defined as a descriptive parameter for steady-state cavity studies. In neither closed-jet, open-jet, nor free-jet water tunnel test sections can the velocity of the flow be expected to be constant throughout even when there is no cavitation head in the test section. This is the natural result of the presence of viscous and gravitational forces encountered in practical studies. However, although the value of $\rho(U^2/2)$ will not be constant throughout the test section for these conditions, within a "core flow" it should not vary by more than a few per cent from the value of $\rho(U_o^2/2)$. Further, the evaluation of this quantity is not difficult. The evaluation of p_k can be accomplished by measuring the pressure within the steady-state cavity being studied, its value being constant over the greater length of the cavity and measurable in a gaseous medium for the extremely low cavitation indices of interest here ($\sigma_k \leq 0.05$), although this may not be true in general for steady-state cavities [2]. The remaining term, p_o, is difficult to evaluate and does not accurately represent the pressure conditions throughout the test section in closed-jet and open-jet water tunnels. In water tunnel testing at low cavitation indices, the value of $(p_o - p_k)$ is very small (the alternative is to make $\rho(U_o^2/2)$ very large, which is not practical), i.e., p_o is of the same order of magnitude as p_k. Therefore, small variations in p_o result in large variations in σ_k. The evaluation of p_o for the closed-jet or open-jet water tunnel must depend on the measurement of the pressure at some boundary point by means of a piezometer tap system. At the velocities which exist in water tunnel studies, such pressure measurements

are not to be relied upon for high accuracy [3]. If the static pressure measurement is in error by only 1/2 per cent of the dynamic pressure, the value of σ_k is in error by $(000.5/\sigma_k)$ per cent which becomes very large for small σ_k. Further, in closed-jet and open-jet water tunnels, the static pressure will vary along the length of the jet due to the formation of a boundary layer in the test section with its accompanying energy losses and will vary across the jet due to hydrostatic pressure effects (assuming a conventional horizontal test section). As a result of these conditions, σ_k defined at any point in the test section of a closed-jet or open-jet water tunnel cannot be considered a reliable index of the cavitation characteristics of the test section as a whole for low cavitation indices. In the free-jet water tunnel, however, these effects are minimized. The jet is surrounded throughout its length and circumference by a constant-pressure gaseous phase (air and water vapor) in which the pressure is easily and accurately determined. The assumption that this pressure is the same as the static pressure at every point within the jet, when there is no cavitation head present, may be slightly in error as noted in references [1, 7, and 10].

Consider now the actual production of a test section flow at very low cavitation indices, i.e., the suitability of the various types of water tunnels for producing the conditions desired. This factor has been discussed previously assuming an ideal fluid with the result that the free-jet tunnel was found to be preferable [4, 5]. The following discussion is based primarily on the physical reality encountered in making experimental studies and assumes that all extraneous cavitation in the test section is to be prohibited. It can be seen that in open-jet or closed-jet test sections which are conventionally horizontal, there are three flow properties of importance as regards the attainment of low cavitation indices in such tunnels. They are: (1) that there is a pressure gradient along the length of the test section due to energy loss in this region; (2) that there is a hydrostatic pressure gradient across the test section; and (3) that there is a dynamic pressure gradient in the region of transition from test section to diffuser, due to the curvilinear flow which occurs in this region. Each of these has the effect of limiting the value of σ_k which can be produced in the test section without resulting in extraneous cavitation at some secondary point. This extraneous cavitation is what may be termed burbling cavitation and consists of small cavities which form in a region of low pressure and collapse as they are carried downstream into regions of higher pressure.

For the case where a closed test section is clear of all obstructions, cavitation will first occur at the top of the transition from the test section to the diffuser, as it is at this point that the static pressure of the flow reaches its minimum value; i.e., there has occurred the maximum energy loss through the test section, there is a minimum pressure due to the hydrostatic effect, and there is a minimum pressure due to the curvilinear flow in this region. For the open-jet type water tunnel this may not be exactly true as shall be mentioned later. If σ_k is evaluated at the centerline of the upstream end of the test section and it is assumed that the cavitation pressure, p_c, for all cavitation equals p_k, the σ_k for this case can be written as

$$\sigma_k = \sigma_{cr_d} = K_1 + K_2 + \frac{\frac{D_o}{2}}{\frac{U_o^2}{2g}}$$

where σ_{cr_d} = the cavitation index on the centerline of the test section at the upstream end when cavitation first occurs at the transition,

K_1 = the head drop due to energy loss in the test section divided by $U_o^2/2g$,

K_2 = the maximum head drop in the transition region due to curvilinear flow divided by $U_o^2/2g$, and

D_o = the test-section depth.

The value of K_1 is dependent on the particular system being considered; however, for the purpose of this discussion it shall be taken equal to its limiting value for a cylindrical test section, which is zero. (It can be shown that by flaring the test section slightly rather than forming it into a cylindrical shape, the net effect of this factor could conceivably be to decrease σ_{cr_d}.) Then

$$\sigma_{cr_d} = K_2 + \frac{\frac{D_o}{2}}{\frac{U_o^2}{2g}} \qquad (1)$$

The value of K_2 is a variable with respect to the particular test installation also, but it should be approximately equal to 0.0165 according to studies reported in section IV-E of reference [6] for closed-jet water tunnels. For

open-jet water tunnels it is to be expected that this value of K_2 would be considerably larger due to the rapid transition from contracting flow to expanding flow which occurs in the pickup region of such water tunnels. Under the most ideal conditions, the value of K_2 would also be zero and $\sigma_{cr_d} = (D_o/2)/(U_o^2/2g)$; however, this would occur only if there were no transition and hence no diffuser.

For the case where there is a streamline body supported in the test section, additional factors become important. The flow cross section is reduced in the region in which the body is located, reaching a minimum value at the point where the body cross section is a maximum when there is no cavitation on the body. The flow is accelerated in passing from the unobstructed region of the test section to this region of minimum flow cross section. This will be accompanied by a pressure drop with the result that cavitation is likely to occur at the top of the test section in this plane. To permit an approximate analysis of this situation, it may be assumed that the body is a rotationally symmetrical one supported on the centerline of a horizontal circular test section, that the velocity is uniform in the plane of minimum flow cross section as well as in the plane at which p_o is measured, and that there is no head loss between the two planes; the latter two assumptions have compensating effects as regards this analysis. Bernoulli's equation and the continuity equation between these two planes are then as follows:

$$\frac{p_o}{w} + \frac{U_o^2}{2g} = \frac{p_t}{w} + \frac{U_t^2}{2g} + \frac{D_o}{2}$$

$$U_o D_o^2 = U_t (D_o^2 - d_m^2)$$

where p_t = the absolute pressure at the top of the plane of minimum flow cross section,

U_t = the speed of the flow in this plane, and

d_m = the maximum body diameter.

Setting p_t equal to p_k, the pressure at which burbling cavitation is incipient, and combining these two equations yields

$$\sigma_k = \sigma_{cr_t} = \frac{\frac{p_o}{w} - \frac{p_k}{w}}{\frac{U_o^2}{2g}} = \left(\frac{D_o^2}{D_o^2 - d_m^2}\right)^2 + \frac{\frac{D_o}{2}}{\frac{U_o^2}{2g}} - 1 \qquad (2)$$

where σ_{cr_t} is the cavitation index on the centerline of the test section at the upstream end when cavitation first occurs at the top of the plane of minimum flow cross section.

The foregoing discussion has been carried out assuming a rotationally symmetrical body supported in the flow; however, within the approximations used, the major portion of this body could be replaced by a steady-state cavitation bubble. This is the true condition for the case of interest. The solid body about which the steady-state cavity forms will be referred to as a cavitation head.

The presence of this cavitation head and the accompanying steady-state cavitation bubble in the flow will also affect the value of σ_{cr} for cavitation at the transition from test section to the diffuser. The pressure-momentum relationship for two planes, one at the upstream end of the test section and one at the downstream end, may be written

$$\int_{A_o} p\,dA + \rho \int_{A_o} U^2 dA = \int_{A_e} p\,dA + \rho \int_{A_e} U^2 dA + F$$

where A = the cross-sectional area of the test-section flow,
o - refers to the upstream plane,
e - refers to the downstream plane, and
F = the drag on the test section and cavitation body.

Assuming that the velocity is uniform over both the upstream and downstream planes and that the pressure is hydrostatically distributed in both planes, the above equation reduces to

$$F = A\,(p_o - p_e)$$

where p_e is the absolute static pressure at the centerline of the downstream plane. Disregarding the energy loss due to the test section itself, the term F then represents the drag on the cavitation body. According to H. Reichardt [7], this drag term can be written as

$$F = f\,\sigma_k A_m\,\rho\,\frac{U_o^2}{2}$$

where A_m = the maximum cross-sectional area of the cavitation bubble described by σ_k, and

f = a shape factor depending on the body shape such that $0.9 \leq f \leq 1.0$ and $f \to 1$ as $\sigma_k \to 0$.

Then $$p_o - p_e = f\,\sigma_k \left(\frac{A_m}{A}\right) \rho \frac{U_o^2}{2}$$

Introducing this factor into Eq. (1)

$$\sigma_{cr_d} = K_2 + \frac{\frac{D_o}{2}}{\frac{U_o^2}{2g}} + f\,\sigma_k \left(\frac{A_m}{A}\right)$$

Setting $\sigma_k = \sigma_{cr_d}$, which is true as the pressure at which cavitation is incipient has been taken equal to that within a steady-state cavity, and solving for σ_{cr_d}

$$\sigma_{cr_d} = \frac{K_2 + \frac{D_o/2}{U_o^2/2g}}{1 - \left(\frac{A_m}{A}\right) f}$$

Taking $f = 1.0$ and noting that $(A_m/A) = (d_m/D_o)^2$, then

$$\sigma_{cr_d} = \frac{K_2 + \frac{D_o/2}{U_o^2/2g}}{1 - \left(\frac{d_m}{D_o}\right)^2} \tag{3}$$

Equations (2) and (3) are expressions for the critical cavitation index for incipient extraneous cavitation at two separate points in the test section. As both are assumed to be undesirable, the test section is operating at maximum efficiency when $\sigma_{cr_t} = \sigma_{cr_d} = \sigma_{cr_b}$, the cavitation index on the centerline of the test section at the upstream end when cavitation first occurs at both the transition from the test section to the diffuser and the top of the plane of minimum flow cross section of a conventional water tunnel. Combining Eqs. (2) and (3) and solving for σ_{cr_b} then yields

$$\sigma_{cr_b} = \frac{K_2 + B}{2} \left\{ (K_2 + B) + \left[4\,(1 - B) + (K_2 + B)^2 \right]^{\frac{1}{2}} \right\} \tag{4}$$

where $$B = \frac{\frac{D_o}{2}}{\frac{U_o^2}{2g}}$$

Hence $$\sigma_{cr_b} \simeq \frac{(K_2 + B)(K_2 + 2)}{2} \quad \text{for small B,}$$

$$\simeq K_2 \text{ for } B = 0 \text{ and } K_2 \text{ small, and}$$

$$= B \text{ for } K_2 = 0$$

Equation (4) has been plotted in Fig. 1 for the arbitrarily selected values of $K_2 = 0.033$, $K_2 = 0.0165$, and $K_2 = 0$.

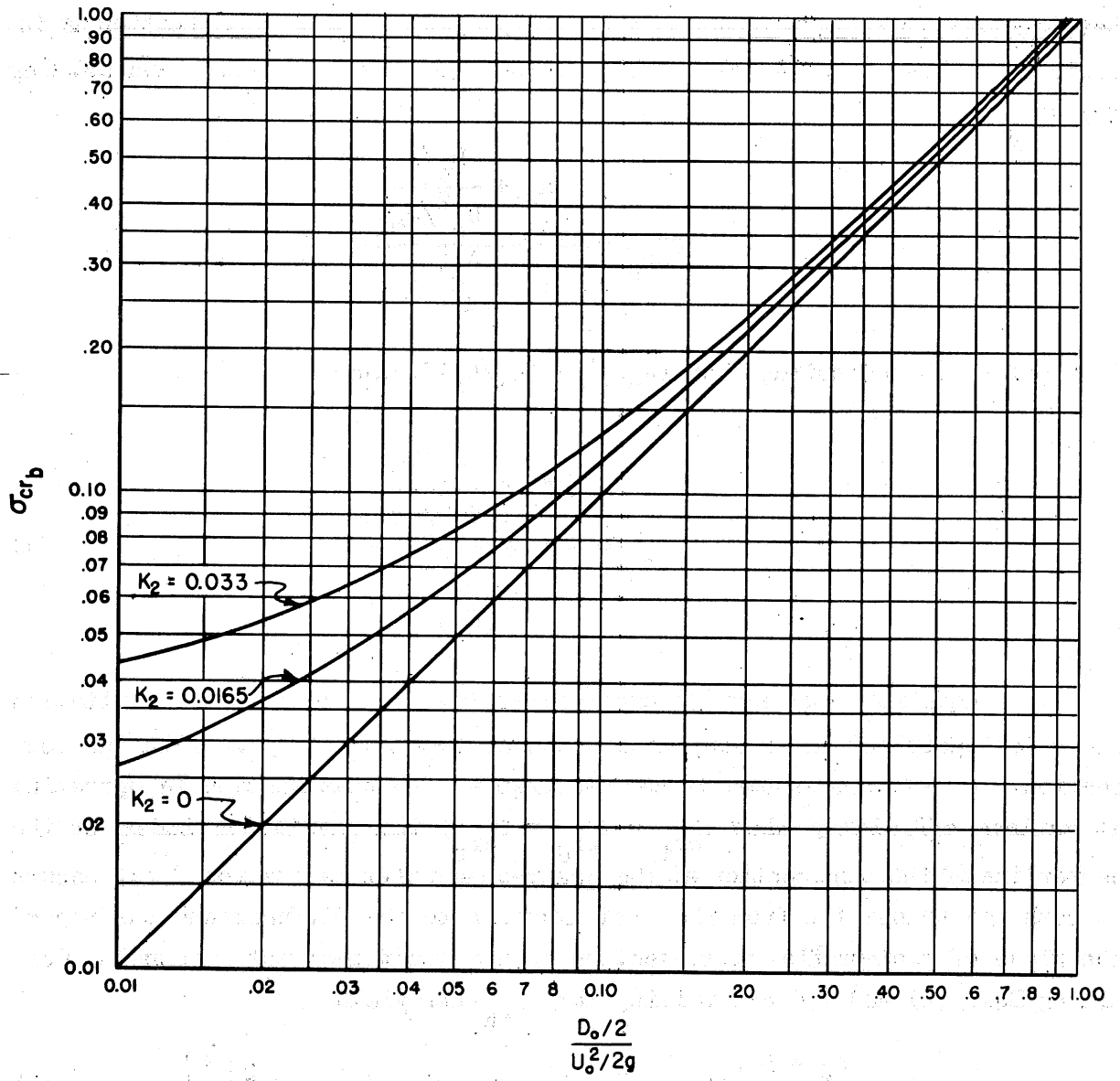

Fig. 1 – Graphical Representation of Equation 4

Solving Eq. (3) for d_m/D_o in terms of $\underline{B}$ gives

$$\frac{d_m}{D_o} = \left[1 - \frac{(K_2 + B)}{\sigma_{cr_b}}\right]^{\frac{1}{2}} \tag{5}$$

where σ_{cr_b} is given by Eq. (4). Equation (5) has been plotted in Fig. 2 for $K_2 = 0.033$, $K_2 = 0.0165$, and $K_2 = 0$.

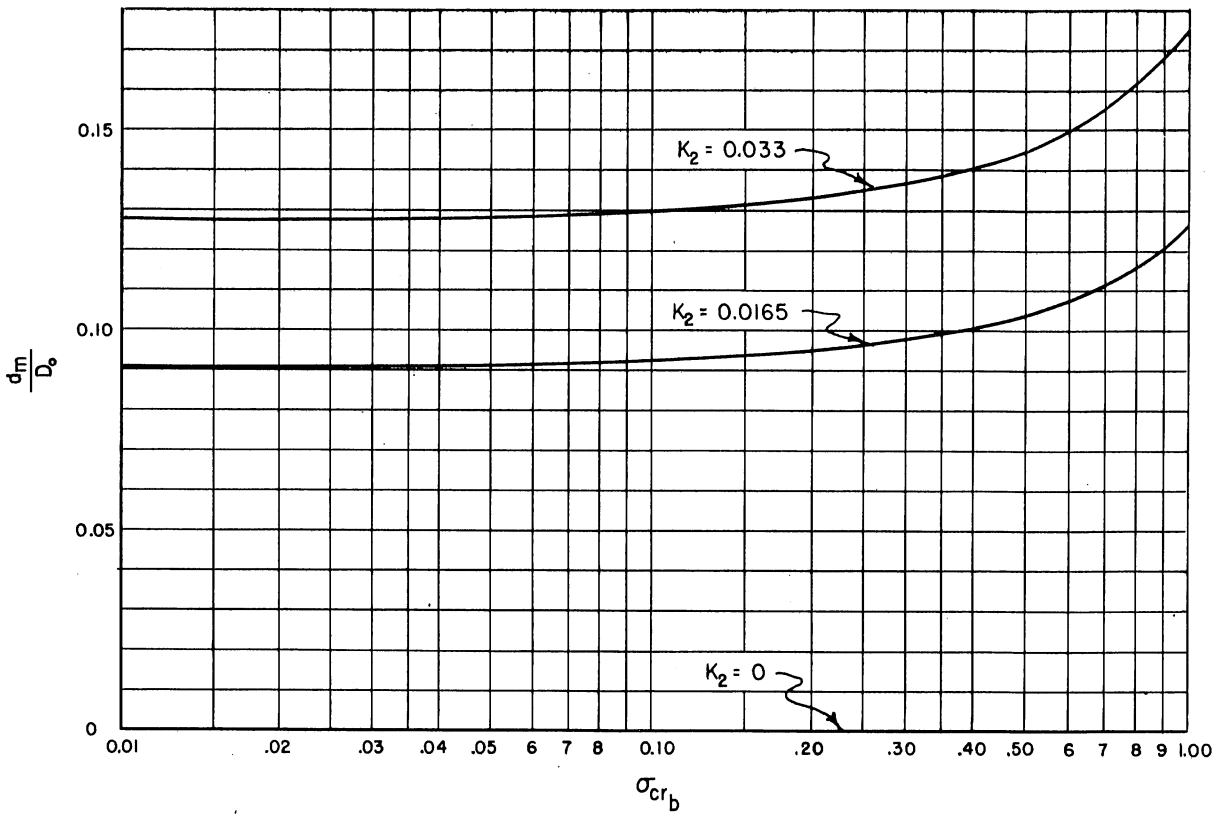

Fig. 2 – Graphical Representation of Equation 5

To illustrate the use of these charts, it is assumed that it is desirable to make cavitation studies at values of $\sigma_k \geq 0.05$ and that the K_2-value for the tunnel will be 0.0165. From Fig. 1, $(D/2)/(U_o^2/2g) = 0.033$ when $\sigma_{cr_b} = 0.05$, and from Fig. 2, $d_m/D_o = 0.092$ when $\sigma_{cr_b} = 0.05$. Now if either D_o, U_o, or d_m is fixed, the other two will be determined also; i.e., assume $U_o = 50$ fps, then

$$D_o = (0.033)\left(\frac{50^2}{32.2}\right) = 2.56 \text{ ft, and}$$

$$d_m = (0.092)\ (2.56) = 0.236 \text{ ft}$$

Figures 1 and 2 illustrate graphically the impracticality of making steady-state cavitation studies at low cavitation indices in closed-jet or open-jet water tunnels. It should be noted that in open-jet water tunnels there is another source of burbling cavitation associated with a much higher σ_{cr} than those discussed above. This consists of the region of shearing action between the jet and the water enveloping it in the test-section barrel [6, 8].

The same components comprise a free-jet water tunnel that comprise open-jet and closed-jet water tunnels except for the diffuser which is impractical at the low cavitation indices at which the free-jet tunnel would be operated. This is easily seen if the physical problem involved is considered in the light of the preceding approximate analysis. The situation is analogous to cavitation in Venturi tubes except that it is further complicated by the fact that the jet is entirely free at an upstream point. The ineffectiveness of the diffuser for free-jet water tunnels has also been verified experimentally by H. Reichardt [1].

It is, however, advantageous to be able to recover the energy of the jet if this can be done by some simple means, and the inherent characteristics of a free-jet water tunnel suggest an alternative method which at first consideration seems very promising. It consists of directing the free jet vertically upward and "catching" it in a reservoir at an elevation at which most of the kinetic energy of the jet has been converted to position energy. While this appears to be the only simple approach to the problem, it too can be seen to have complications. Not all of the water will reach the upper reservoir because there is considerable spray from the surface of the free jet as can be seen from Fig. 14 and the photographs of reference [9]. Further, a certain amount of splash back from the reservoir is inevitable. The result is that an auxiliary pumping system would be necessary to dispose of this water that failed to be caught by the reservoir. This method of regaining the jet energy also places restrictions on design and operation of the water tunnel if it is to be at all effective. That is, the reservoir height must be designed for a specific jet speed and the water tunnel operated at that speed. The net efficiency of such a method is still questionable, and it appears physically preferable that the energy of the jet be considered a permissible energy loss. The head loss in a good recirculating open-jet or closed-jet water tunnel may be taken as $0.2\ (U_o^2/2g)$ [6]; hence, in a free-jet tunnel in which the head loss in the jet alone is equal to $U_o^2/2g$, the total head

loss is over five times greater than that in a conventional water tunnel. This means that, for comparable dimensions and velocities, the power input to a free-jet water tunnel must be over five times that of an open-jet or closed-jet tunnel and that the rate of temperature rise of the flowing water (assuming that it is recirculating) is commensurately greater also.

It should also be noted, although it is obvious, that gravity does have an effect on the flow in a free-jet test section as well as in open-jet or closed-jet test sections but of a different nature. In a free-jet test section, gravity affects the configuration and speed of the jet. Assuming one-dimensional flow, the effect of gravity on the speed of a horizontal jet can be written as

$$\frac{U}{U_o} = \left(1 + \frac{1}{Fr^2}\right)^{\frac{1}{2}} \tag{6}$$

where U = the speed of the jet at a distance L measured along the contraction axis from its downstream face, and

Fr = the Froude number = U_o^2/gL.

Similarly the effect of gravity on the speed of a free jet directed upward or downward can be written as

$$\frac{U}{U_o} = \left(1 \pm \frac{2}{Fr}\right)^{\frac{1}{2}} \tag{7}$$

the positive sign applying to the jet directed downward. The effect of gravity on the configuration of a horizontal free jet is to cause the jet to bend downward with distance from the nozzle face according to the equation

$$\frac{y}{L} = \frac{1}{2Fr}$$

where y is the distance the jet centerline falls below the contraction axis in the axial length L.

For a vertical free jet, the effect of gravity on the diameter of a jet of circular cross section is given by

$$\frac{D}{D_o} = \left(\frac{Fr}{Fr \pm 2}\right)^{\frac{1}{4}} \tag{8}$$

the positive sign applying to the jet directed downward, where D is the jet diameter at a distance L downstream of the nozzle exit. For the purposes of comparison, it is assumed that for a practical maximum $L = 5D_o$ in Eq. (8) which can then be written as

$$\frac{y}{D_o} = \frac{5}{2Fr} \tag{9}$$

Equations (6) and (7) are plotted in Fig. 3, and Eqs. (8) and (9) are plotted in Fig. 4. It can be seen from these figures that from the standpoint of speed, the horizontal jet is preferable; but from the standpoint of configuration, the free jet directed vertically downward is to be preferred. This is a one-dimensional viewpoint, however, and it is intuitively obvious that the horizontal free jet will have both a velocity gradient and a pressure gradient across the jet; for the two-dimensional case, this fact has been investigated by A. H. Armstrong and E. P. Hicks [10]. This means that while the mean velocity of the horizontal jet is less affected by gravity than that of a vertical one, there exist in the horizontal jet nonsymmetrical distortions of velocity and pressure fields which do not occur in the vertical jet. Further, the jet directed vertically downward is to be preferred over the jet directed vertically upward unless it is mandatory that at least a part of the energy of the jet be regained. This is true because in a jet directed vertically downward, the spray from the jet will not create an additional pumping problem, and because the effect of gravity on the reentrant jet found to occur at the rear of steady-state cavitation bubbles [7] in a jet directed vertically upward would be to cause this jet to fall all the way forward and strike the front of the bubble which would be very undesirable.

Another factor which must be considered in the design and operation of a free-jet water tunnel is the entrainment of air by the free jet. That this will be a problem is also intuitively obvious. The mechanism of air entrainment will take two forms--air will be entrained through the surface of the jet and considerable air will be entrained downstream of the test section where the jet strikes the free water surface in the "pickup" region. In addition to this air entrainment, there may be air released from solution in the region of low pressure which comprises the test section. This latter problem also exists in open-jet and closed-jet water tunnels, in which case it is necessary only to "resorb" this air downstream of the test section. The combination of air being entrained and air being released from solution would require selective resorption and separation if the air content of the water

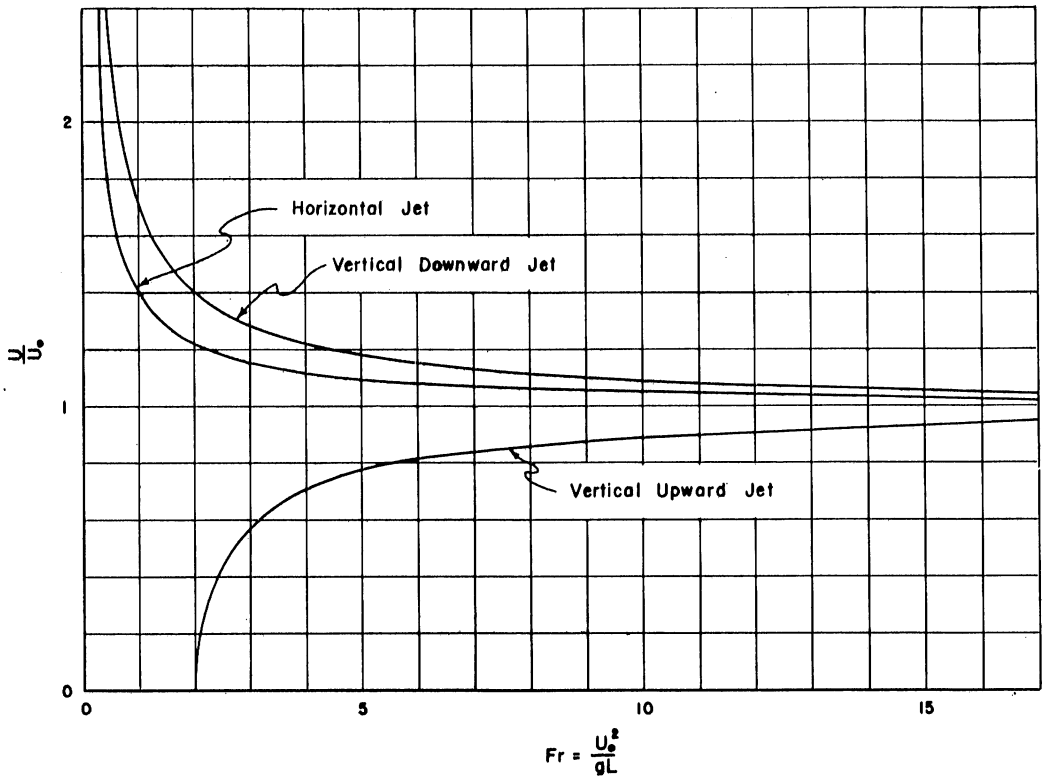

Fig. 3 — The Effect of Gravity on Free-Jet Speed

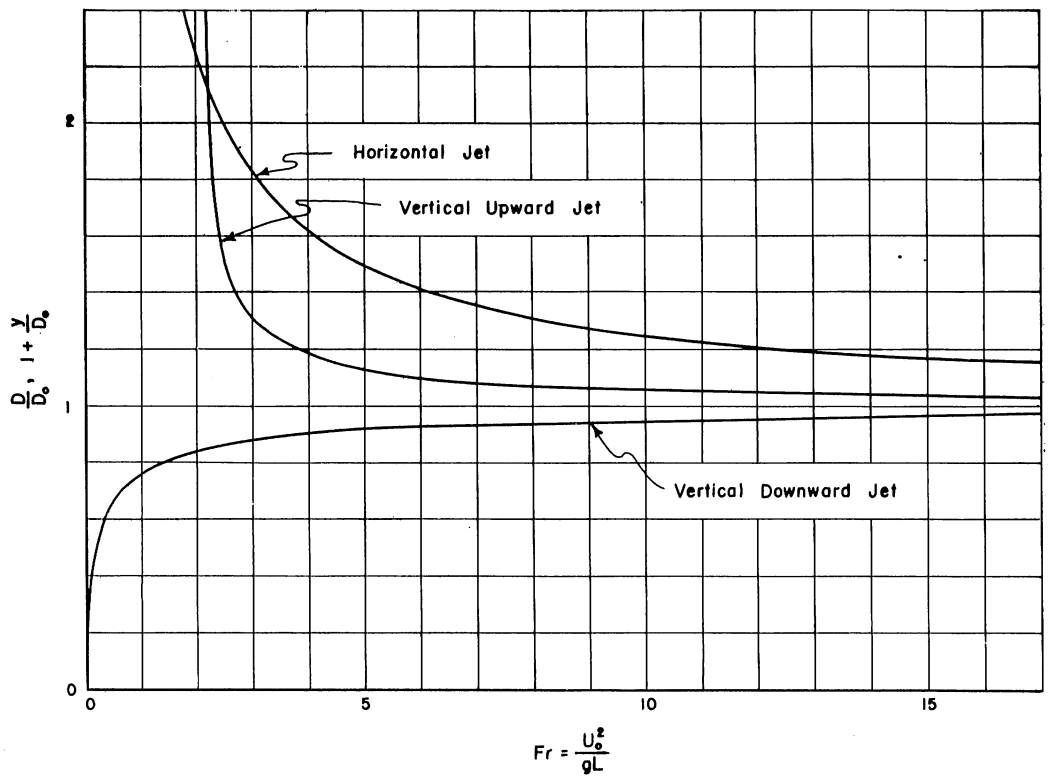

Fig. 4 — The Effect of Gravity on Free-Jet Configuration

is to be controlled; however, the difficulties in achieving such ideal conditions might well prove insurmountable. A more promising approach would be to separate from the flow all of the air which was in bubble form just downstream of the test section so that an equilibrium condition might be attained in which the air content of the test-section flow would be at or near saturation for the test-section pressure and temperature. The mechanism by which air bubbles could be separated from the flow might take any one of a number of forms, such as discharging the jet into a large tank and relying on the buoyant forces to separate the air bubbles and water; supplementing this by screens in the tank to diffuse the jet and collect fine bubbles; and collecting the air at certain points by means of natural tunnel components such as guide vanes or special components such as screen funnels which would collect the air in a core flow, and then actively sucking the air out of the flow. The use of a large tank would probably be the most effective and the simplest, particularly if it incorporated a device just downstream of the test section which would break up the jet into a fine spray. This would have two advantages in that the velocity distribution in the tank would then be more uniform and hence it would be more effective in separating the flow and secondly, air bubbles would not be driven as deeply into the water in this tank where they would be of commensurately smaller size and hence more difficult to separate.

The latter portion of this section has been devoted to the discussion of some of the problems which should be expected in the operation of a free-jet water tunnel and which the designer must allow for; some of these problems will be discussed further in connection with the experiments described in the following section. The fact remains, however, that the free-jet water tunnel is the only available means for studying true steady-state cavitation bubbles at low cavitation indices.

III. EXPERIMENTAL APPARATUS

As has been previously noted, the experimental equipment consisted of a small, pilot, free-jet water tunnel of a very general design, and the experimental procedure consisted largely of general observations of this tunnel in operation. Figure 5 is a drawing of this water tunnel as it was initially set up with the jet directed vertically upward and the flow recirculating. Figures 6 and 7 are photographs of the tunnel in its two alternate forms which shall be mentioned later. The basic features are: the two large reservoirs each 18 inches in diameter and approximately 2-1/2 ft long; the monitor arm

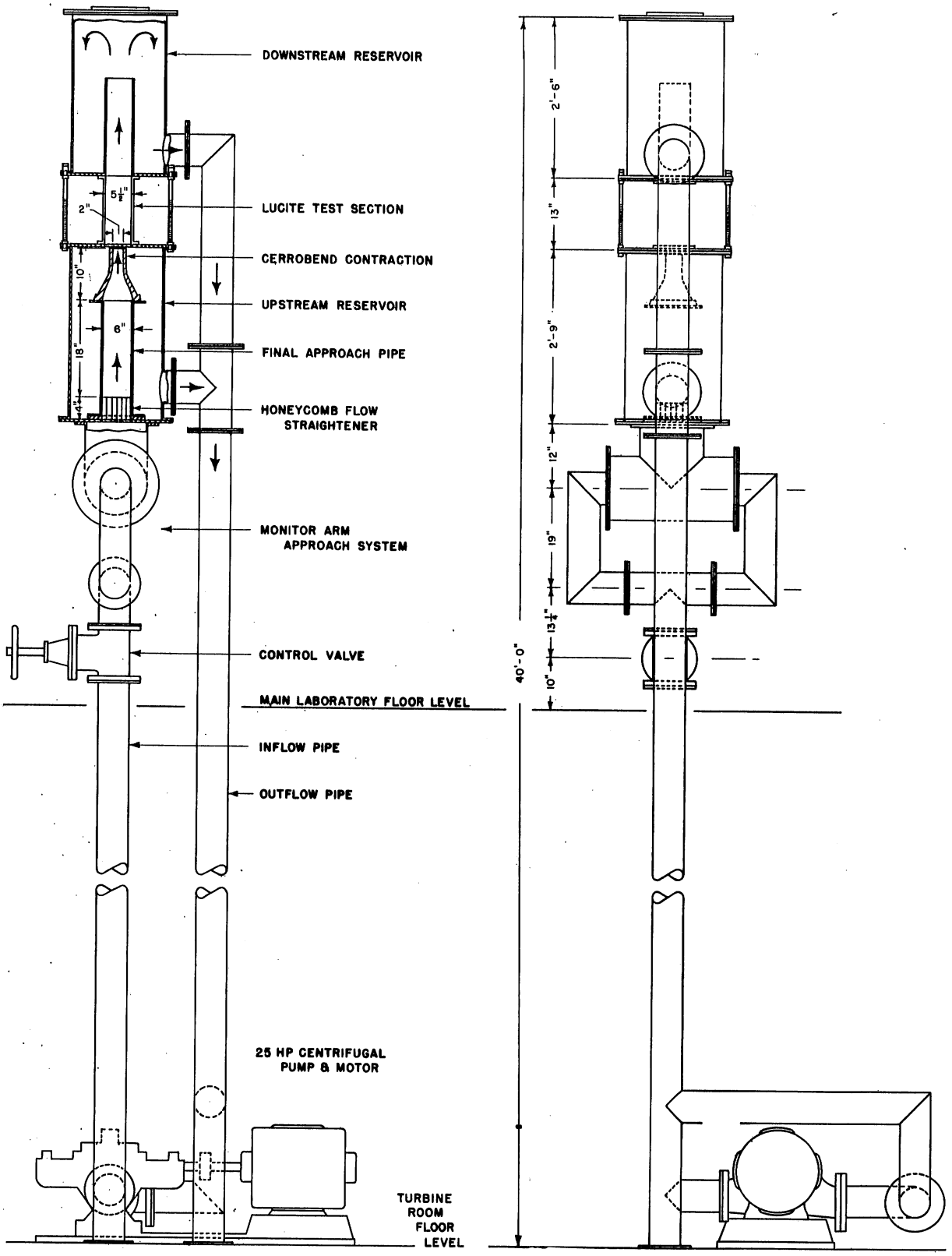

Fig.5— The 2– Inch Free Jet Installation with Jet Directed Vertically Upward

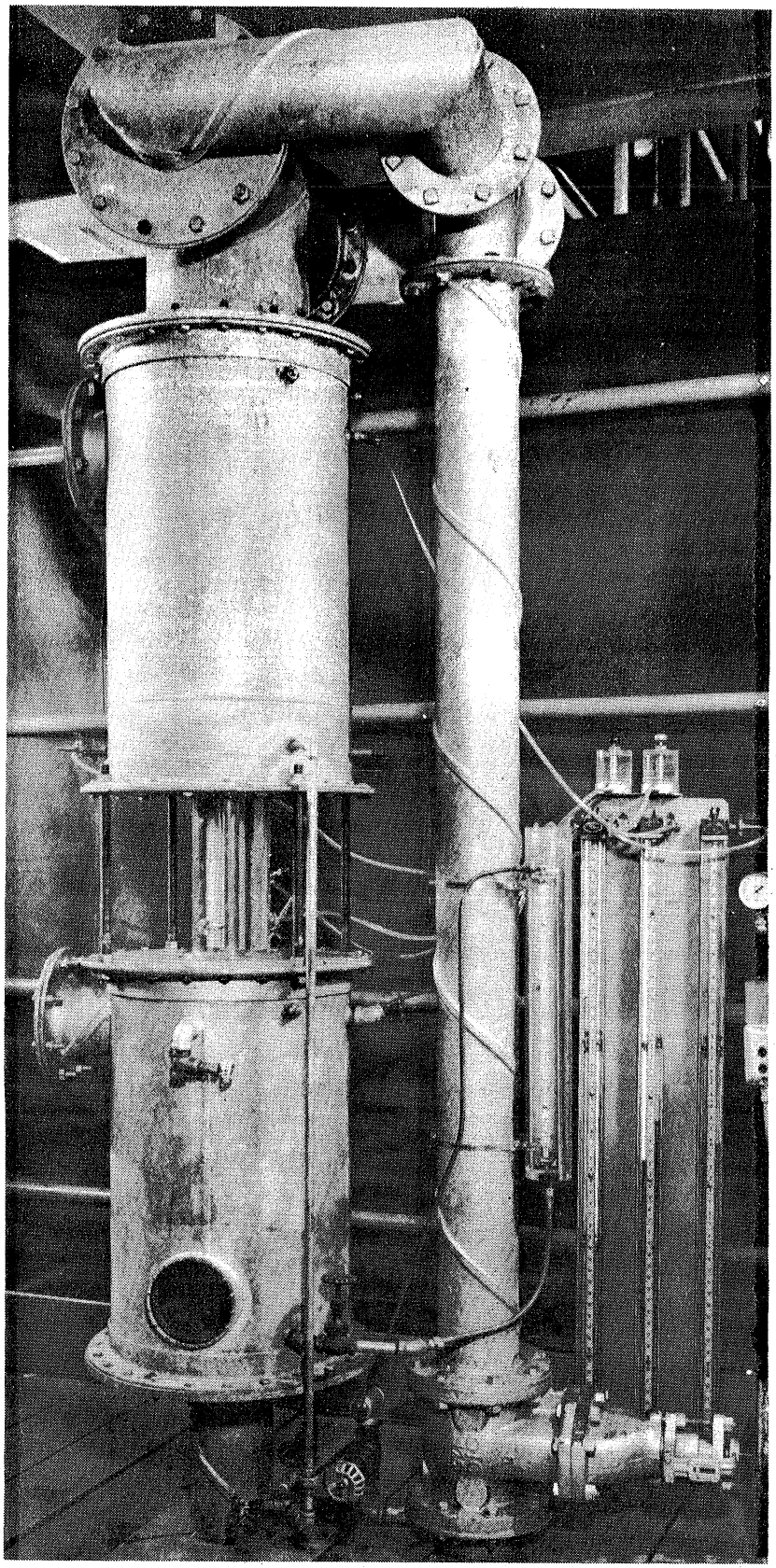

Fig. 6 - Test-Section Region with Jet Directed Vertically Downward

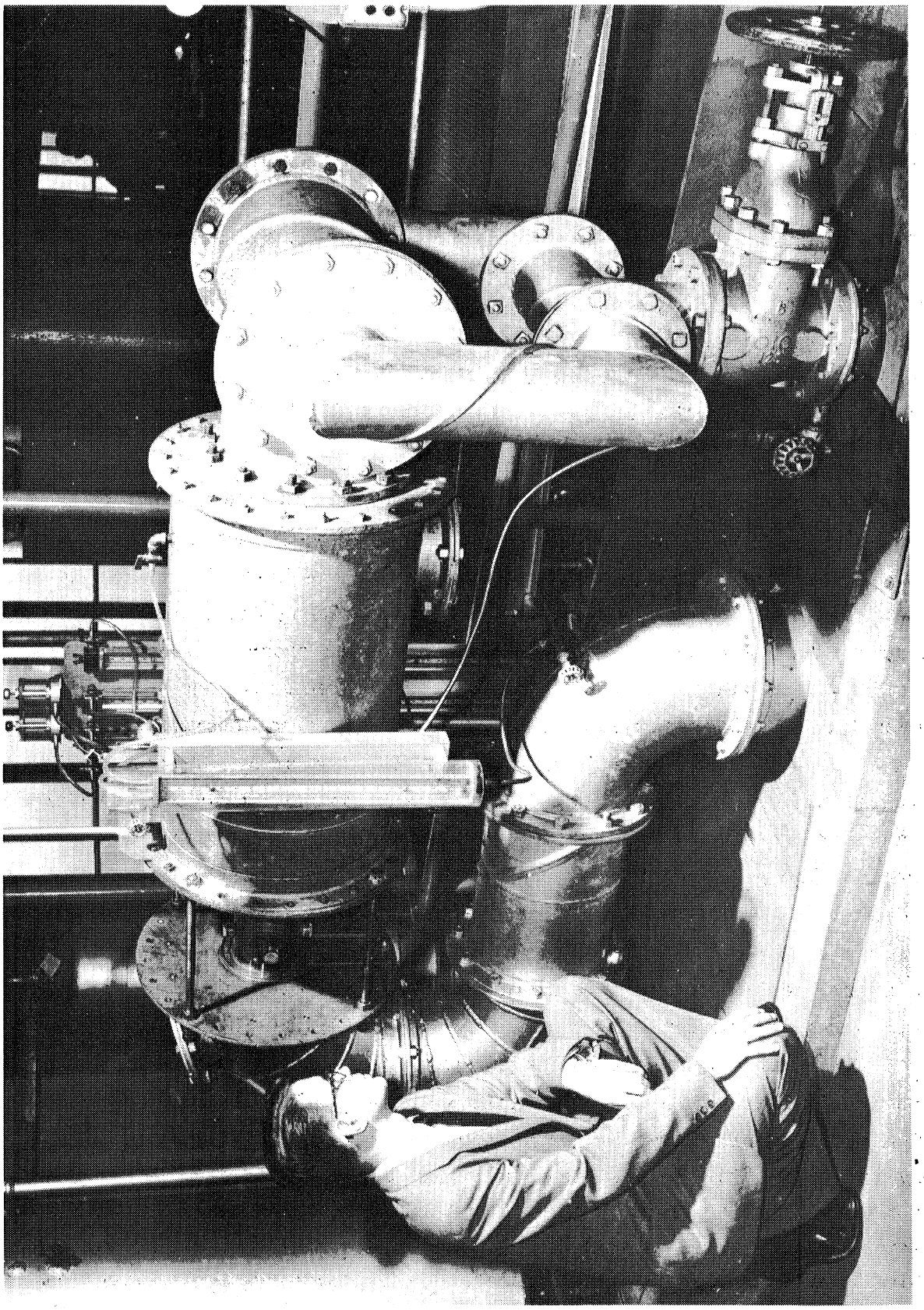

Fig. 7 — Test-Section Region with Jet Directed Horizontally

approach piping (including the 12-in. T-section which served as a stilling zone) which permitted orienting the jet in a vertically upward, vertically downward, and horizontal direction with a minimum difference in the conditions to which the approaching flow was subjected; the control valve which was a standard 6-in. gate valve; the approach pipe which was mounted within the upstream reservoir, was 22 in. long, had an accurately machined inside diameter of 6 in., and had an upstream end fitted with a 6-in. aluminum sleeve for the purpose of locating turbulence screens; the nozzle or contraction which shall be mentioned further; the test section proper which consisted of a section of standard 5-1/2-in. inside diameter Lucite tubing of 1/4-in. wall thickness; the pump which was a standard single-stage centrifugal type pump rated at 1200 gpm at 60 ft of head; and the standard 6-in. lightweight pipe which formed the necessary connecting conduit.

The only refinement in design and finish was that incorporated in the contraction. In selecting a contraction design for a free-jet water tunnel, several factors should be considered. Because of the extremely low pressures at which a free-jet water tunnel can be operated, it is mandatory that the boundary pressure be a monotonically decreasing function of the distance from the upstream face of the contraction in order to eliminate the possibility of cavitation occurring within the contraction. The use for the jet should be considered in determining the type of cross section employed; i.e., for general purposes and particularly for the study of rotationally symmetrical steady-state cavities, the circular cross section would be preferable, and for two-dimensional studies, a rectangular cross section would be preferable. The general advantages of a circular cross section are that it is inherently the most stable form of a free jet [11] and that the circular cross section of the contraction presents the least possibility of extraneous flow disturbances occurring within the contraction which might cause flow separation and cavitation. In view of the foregoing considerations, a contraction of circular cross section was selected; the design of this contraction had previously been carried out for a proposed 60-in. closed-jet water tunnel on which model studies have been made at the St. Anthony Falls Hydraulic Laboratory [6, 12]. This contraction had a length of 5 exit diameters and an area contraction ratio of 9. Because of the small scale involved (downstream diameter = 2 in., upstream diameter = 6 in., and length = 10 in.), it was not feasible to machine readily and accurately the inside of the contraction. Consequently, a form was machined to the dimensions of the interior of the contraction and the contraction cast of Cerrobend (a commercial alloy of low

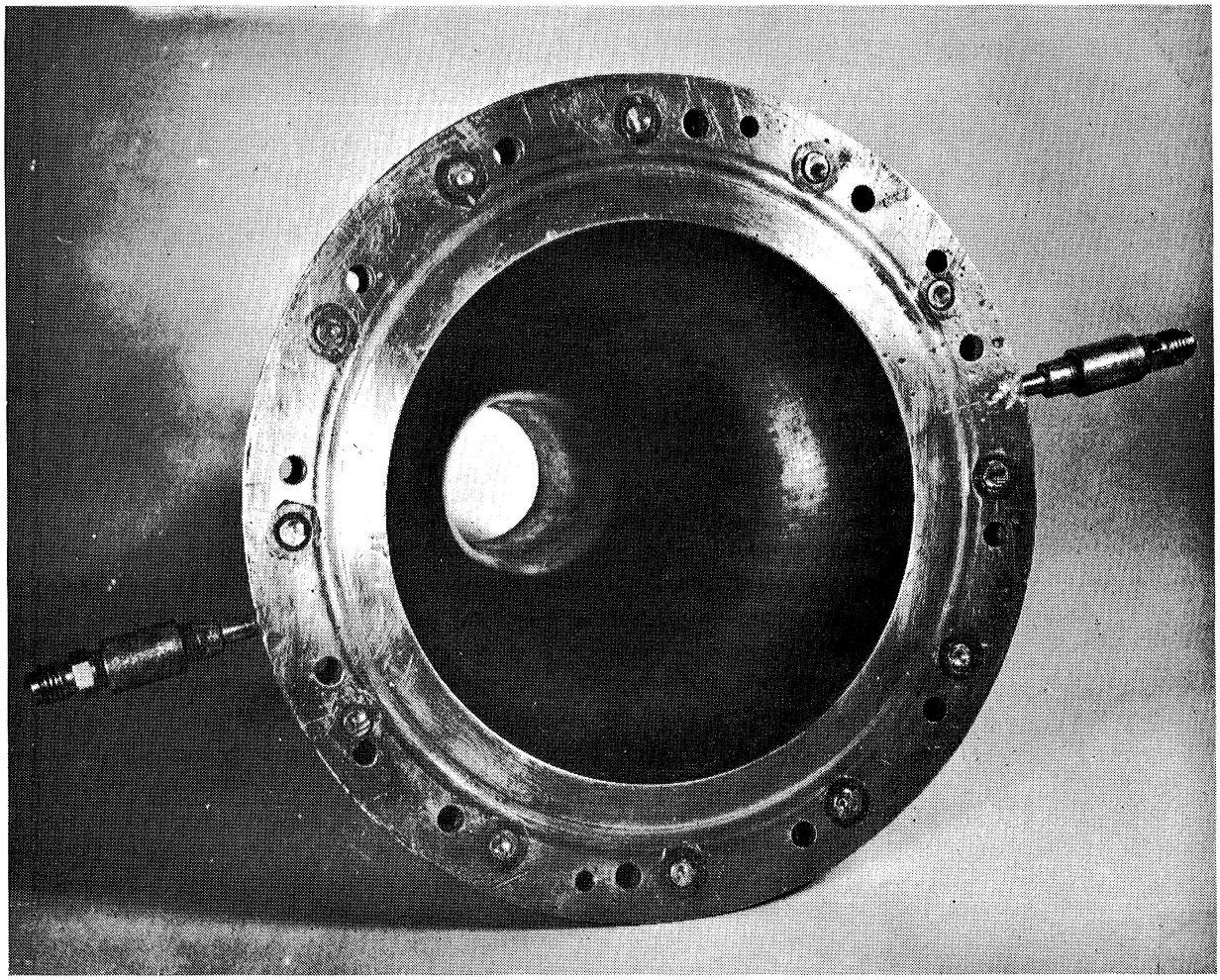

Fig. 8 – Molded Cerrobend Contraction

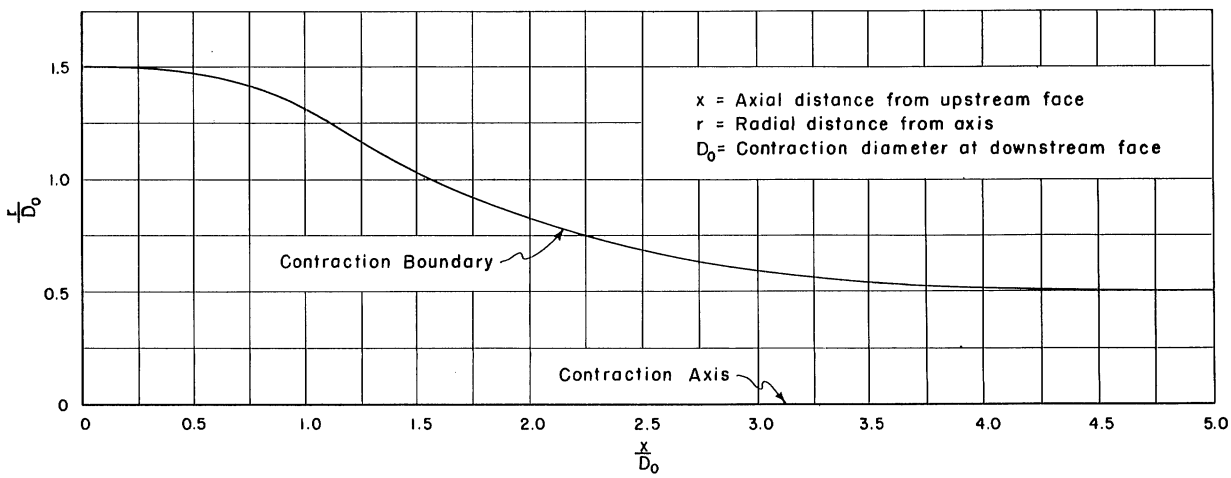

$\frac{x}{D_0}$	0.00	0.25	0.50	0.75	1.00	1.25	1.50	1.75	2.00	2.25	2.50	2.75	3.00	3.25	3.50	3.75	4.00	4.25	4.50	4.75	5.00
$\frac{r}{D_0}$	1.500	1.495	1.470	1.409	1.308	1.172	1.040	0.928	0.834	0.756	0.692	0.640	0.600	0.569	0.546	0.528	0.516	0.507	0.502	0.500	0.500

Fig. 9 – Contraction Boundary Profile

melting temperature) about this form. As the Cerrobend is extremely soft, it was then a simple matter to finish the interior of the contraction by polishing. Figure 8 is a photograph of the contraction, showing also the two piezometer connections for use in making velocity determinations; Fig. 9 is a sketch of the cross section of the contraction with the offsets from the centerline to the boundary curve tabulated.

It early proved necessary to employ viewing windows in the test section which made a solid contact with the jet in order to view the interior. These viewing windows were machined from solid blocks of Lucite with an inside diameter of 2 in.; an outside diameter of 5-1/2 in., the inside diameter of the test section; each covered 0.117 of the jet circumference (included angle of 42^{o}); and they were 13 in. long. These viewing windows are shown in the photograph of Fig. 10, which also shows the brass rods that held them in place in the test section. They were mounted parallel to the jet centerline (no provision being made for gravitational effects on the jet) and diametrically opposite when both were used.

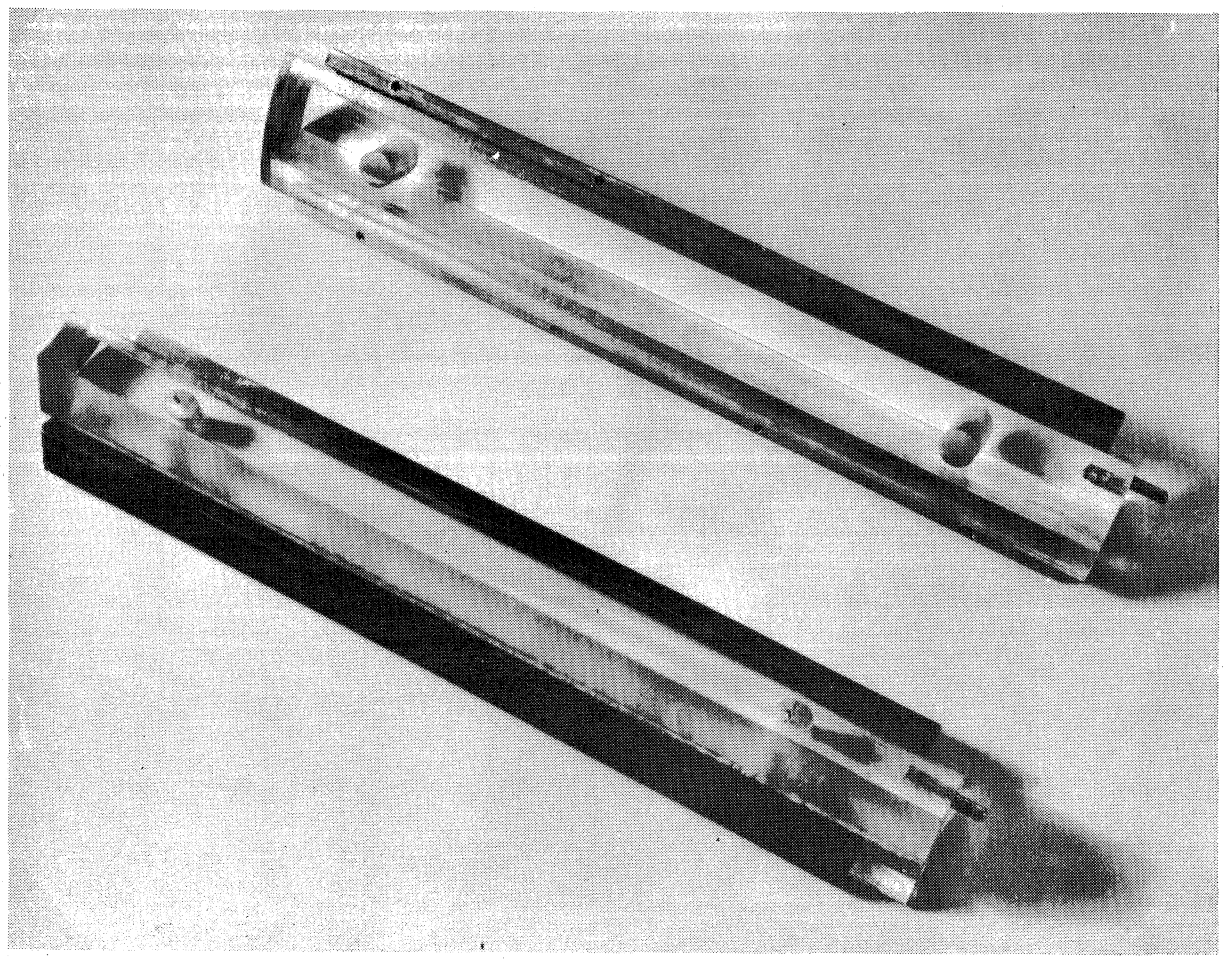

Fig. 10 - Lucite Viewing Windows

Figure 11 is a photograph of the various types of cavitation heads and support systems employed. The struts were hand made from brass stock with a maximum centerline thickness of 1/16 in. and were symmetrically sharpened to a knife edge. The support rods were made from 1/8-in. diameter stainless steel or brass rod and tubing. The cavitation heads, limited to cone forms of 30°, 45°, 60°, and 90° included angles, were machined from stainless steel and push fitted to the rods. Stainless steel 18-gage hypodermic needle tubing was used to form the gage line through the strut of forms D and E which were equipped with piezometer taps to measure cavity pressures.

Figure 12 is a photograph of the Pitot cylinder and Pitot tube used to make total head traverses of the jet. The Pitot cylinder and Pitot tube proper were formed of hypodermic needle tubing which had an outside diameter of 0.049 in. and an inside diameter of 0.033 inches. The nose on the Pitot tube was made from this same tubing with the leading edges rounded by hand polishing. The tap in the Pitot cylinder was drilled to a 1/32-in. diameter. The support guides and positioning mechanism were machined from brass and threaded to fit into sockets on the Lucite test section. The tube and cylinder were positioned by turning part A which was fixed laterally but was threaded to part B, which in turn was silver soldered to the hypodermic needle tubing; these parts are shown slightly separated for the Pitot cylinder. The relative position of the tap on either tube or cylinder with respect to some reference position was given merely by counting the number of turns of part A between positions and multiplying by 0.050 in., the lateral movement per turn.

The viewing windows, strut type E, the Pitot tube, and the contraction are all shown in their attached positions with respect to the test section in Fig. 13. The remainder of the tunnel serves the sole purpose of providing this section with water at the desired rates and ambient pressures.

The gages used (to measure the velocity, absolute pressure in the test section, differential pressure between the test section and the interior of cavitation bubbles, and the total head of the jet) were of the simple, U-tube, differential manometer type. The gage fluids used were mercury, a commercial gage fluid of specific gravity 2.95, and water. The value of the term $(p_o - p_k)/w$, which occurs in the expression for σ_k, was measured directly using water as the gage fluid. As the river water used in the tunnel was always within a few degrees of the freezing point at the time of these tests and the room temperature was near 70° F, this particular gage was equipped

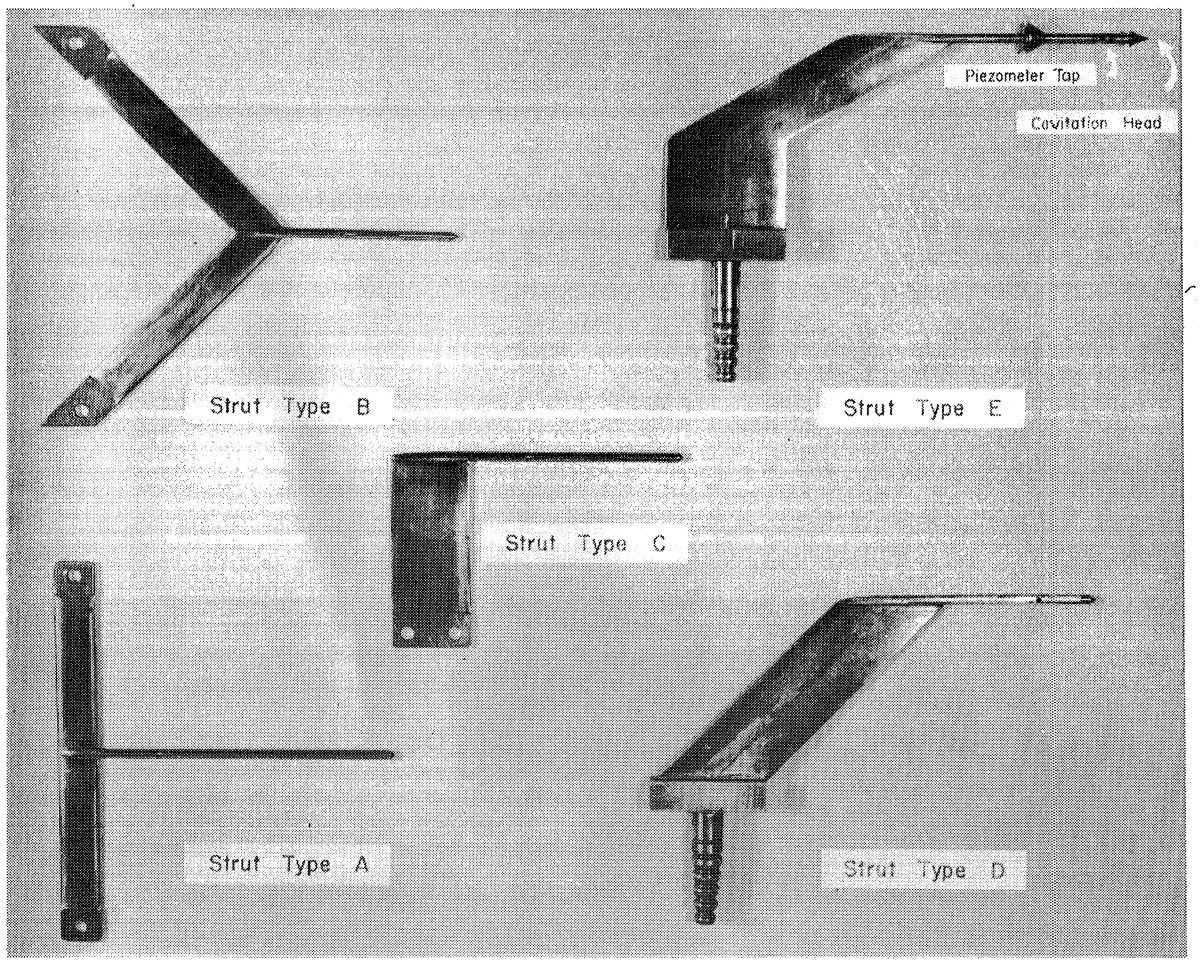

Fig. 11 – Cavitation Body Installations

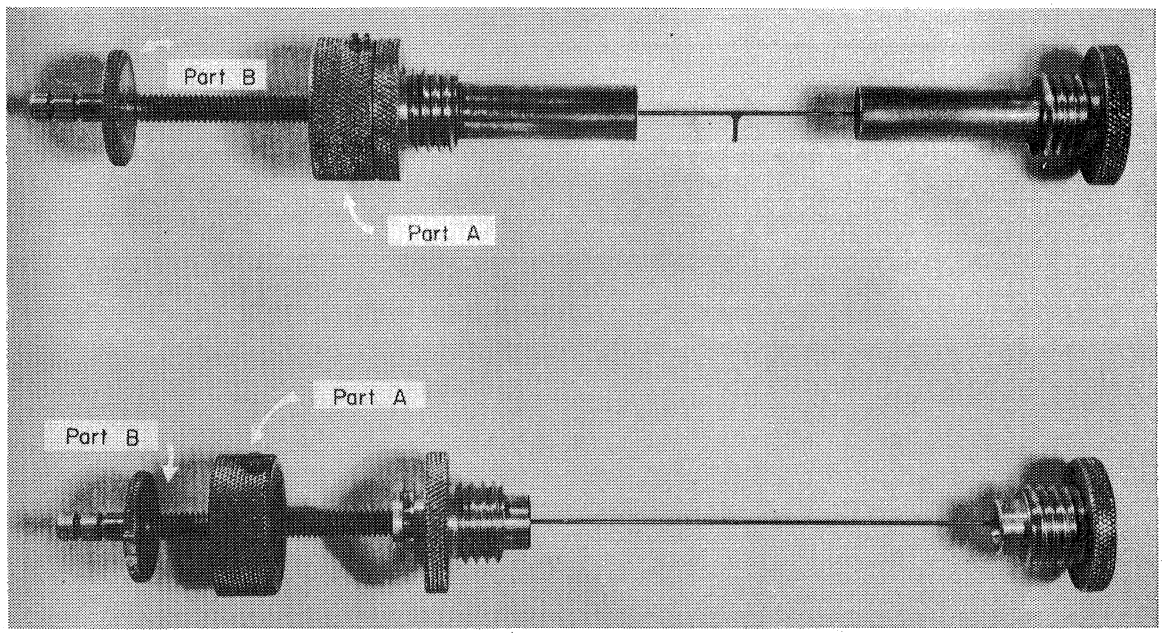

Fig. 12 – Pitot Tube and Pitot Cylinder

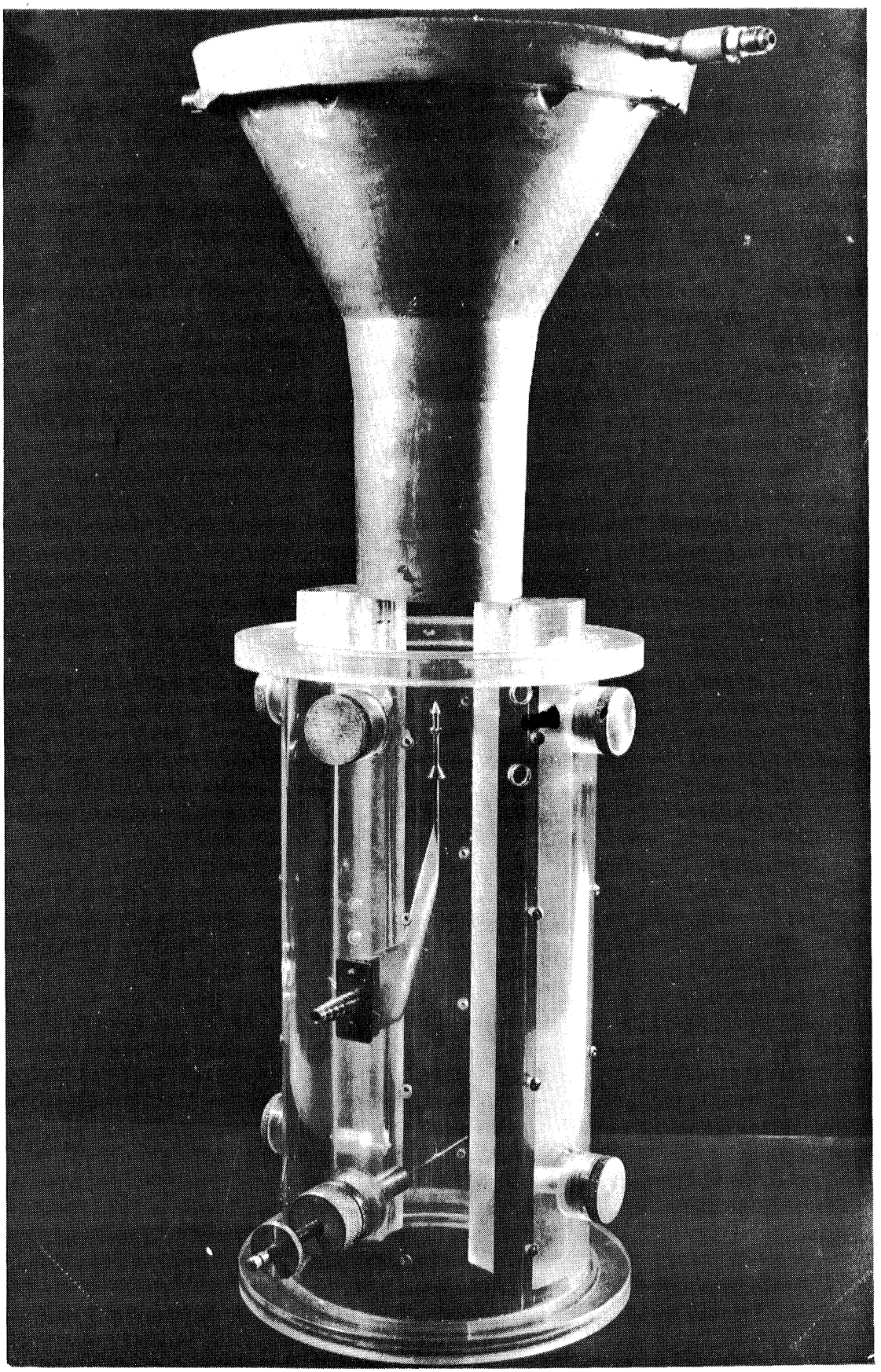

Fig. 13 - Assembled Test Section and Contraction

with a cooling jacket through which water from the tunnel was circulated to prevent the water in the gage from boiling.

The tunnel as shown in Fig. 5 was modified in several ways during the progress of testing. For reasons which shall be explained later, the tunnel circuit was converted to a non-recirculating system in which the suction side of the pump was connected to the main supply channel of the Laboratory and the discharge pipe from the test-section region was led into the tailrace of the Laboratory's turbine room; at this point the water level was approximately 35 ft below the test section and 50 ft below the water level in the supply channel. This modification was made at the same time that the test-section region was reoriented to form a free-jet water tunnel with the jet directed vertically downward as shown in the photograph of Fig. 6. The final modifications consisted of reorienting the test section so that the free jet discharged horizontally and replacing that portion of the tunnel downstream of the test section proper as shown in Fig. 7.

IV. EXPERIMENTAL PROCEDURE AND RESULTS

The experimental procedure used can best be described by considering it in three separate divisions as follows:

(1) Studies carried out with the jet directed vertically upward and with the flow recirculating.

(2) Studies carried out with the jet directed vertically downward and with the flow non-recirculating.

(3) Studies carried out with the jet directed horizontally and the flow non-recirculating.

As noted previously, the original setup of the 2-in. free-jet water tunnel was as shown in Fig. 5. The water used in the tunnel was obtained from the city water supply and recirculated by means of the centrifugal pump. Test-section pressures below atmospheric were obtained by filling the entire tunnel with water, sealing it off from the atmosphere and the city water supply, and then draining part of the water out from the bottom of the discharge leg. As a temporary expedient, this proved satisfactory even though this resultant pressure gradually increased because of vacuum leaks in the system. It is extremely difficult to seal such a system against the high vacuums employed in free-jet water tunnel research, and it is even more difficult to determine

the location of the high vacuum leaks that do occur. For operation, the stagnant water level was set slightly below the nozzle exit, the pump turned on (which had only one speed), and the valve opened as rapidly as possible. The jet discharged from the contraction through the test section and into the downstream reservoir (above the test section) where it was collected. There was a combination of pumping action from this reservoir and natural drainage into the lower reservoir which kept the water level in the upper reservoir comparatively low. The velocity of the jet was determined by connecting a differential manometer across the piezometric pressure near the upstream face of the contraction and the test-section pressure.

Observations made on these initial tests led to several general conclusions. It was immediately apparent that there was considerable spray from the jet surface which struck the sides of the test section and the riser extending into the upper reservoir. In this case the spray simply drained down through the test section into the lower reservoir; however, as has been mentioned previously, if the vertically upward jet were designed to regain energy, it could now be stated as an experimental fact that an auxiliary pumping system would be required to dispose of this spray. Another factor mentioned previously immediately became experimentally evident; that was the entrainment of air by the flow. The most extreme case was that in which the test-section pressure was at or near atmospheric pressure. In this case the air entrained in the water acted to increase the effective volume of the water sufficiently to cause the water level in the lower reservoir to rise above the nozzle exit and submerge the jet; the large air content of the flow caused the centrifugal pump to become air locked and hence effectively stopped the flow entirely; the jet expanded rapidly after leaving the contraction because of the expansion of air bubbles within the jet in this region of comparatively low pressure; and the jet took on an almost white appearance indicating very poor optical properties. These effects were apparent almost instantly when the test-section pressure was near atmospheric. As the initial test-section pressure was decreased, the effects became less pronounced and required a progressively longer time to become evident. At very low test-section pressures (near the vapor pressure of the flowing water), the jet appeared to be very milky and expanded slightly upon leaving the contraction, but the total air content was reduced sufficiently so that the contraction never became submerged and so that it took a much longer time before the pump became air

locked. These are all relative statements which are not intended to give specific information concerning the air entrainment problem but only to emphasize the fact that it exists. The reduced effects apparent at the lower test-section pressures can be attributed to the fact that the bubbles carried from the reservoir to the pump in the latter case undergo a relative ambient pressure increase from five to ten times that of the former case, and this ratio is increased even further when the flow passes through the pump. In addition, the bubbles are composed largely of water vapor which condenses in the high pressure regions, leaving only a small air core to be recirculated; hence in re-expanding in the low pressure region of the test section following the contraction, they reach only a fraction of their initial size. This reduction of the effects of air entrainment at low test-section pressures is gratifying because it is mainly at these low pressures that a free-jet water tunnel would be operated. However, if it is intended that the tunnel be operated at pressures near atmospheric and artificial cavitation produced by introducing a stream of air behind a body, the effects of air entrainment will be at their maximum. Further, the large bubbles should be comparatively easy to separate from the flow, whereas the small ones which occur in all cases would be the most difficult.

Consideration was given to incorporating an air bubble separator in the 2-in. free-jet water tunnel system which would separate the bubbles from the flow by using the buoyant forces on the bubble in a large tank [13]. However, the size of the tank was limited by the space available for it, and analytic considerations indicated that under the available conditions the minimum bubble size separated would be comparatively large and consequently there would be little if any actual benefit derived. Some cursory experiments were carried out in a 2-in. diameter Lucite pipe, 36 in. long, to determine the effectiveness of using screen cones and centrifugal forces to create a core flow of highly concentrated bubbles in the pipe which could then be sucked off. A mixture of air bubbles and water was introduced at the top of the pipe by attaching an ejector at this point to the city water supply and the atmosphere, and this mixture flowed downward through the pipe. An auger-shaped device was inserted into the tube resulting in helical flow through the tube. This in turn resulted in the bubbles being collected in a core flow at the center of the pipe due to the centrifugal forces set up. The other method considered employed fine screen (40 mesh) truncated cones placed in the pipe pointing downstream. The diameter of the downstream opening through which

the core flow passed was 1/4 inch. The clear water passed through the pores of the screen, whereas the bubbles were withheld and shunted through the large opening at the tip. The best results were obtained when a single cone was used having a small included angle (15°), although this would depend on the flow-through velocity. Combining the helical flow with the screen cones produced results inferior to those obtained using each separately. The advantage of the screen cone method is the comparatively short distance required for the separation to take place. Both methods would require an auxiliary system capable of actively sucking off this core flow, and it is still questionable as to what value they would have in separating the very fine bubbles which cause "milky" flow. As a consequence, the alternative of converting the 2-in. water tunnel into a non-recirculating system was employed. At the same time, in order to eliminate as much as possible the detrimental effect of gravity on the flow, the test section was reoriented such that the jet discharged vertically downward.

It should also be mentioned here that the gate valve served only as a shutoff valve when the tunnel was operated at ambient test-section pressures near the vapor pressure of the flowing water; any attempt to use it to throttle the flow resulted in cavitation at the valve which was carried over into the test section.

It was with the jet directed downward and with the system non-recirculating that the major portion of the experimental work was carried out. Under these conditions it was not necessary to make use of the pump, as velocities up to 50 fps in the jet could be obtained from gravity flow; although it would have been possible to obtain velocities near 85 fps by combining the pump with gravity flow, it did not seem warranted. Test-section pressures below atmospheric were easily obtained, as the free jet discharging downward into the waste water pipe acted as a large aspirator and very quickly reduced the pressure within the test section to values as low as 0.5 in. of mercury absolute. Pressure control was then obtained by placing a valve between the test section and atmosphere through which air could be bled into the test section in order to maintain pressures above this minimum. The velocity of the flow was determined by the same means as for the vertically upward jet.

The initial studies with this system involved the jet surface. The problem was to determine whether or not viewing windows contacting the jet would be a necessary feature of a free-jet water tunnel. To accomplish this,

high-speed photographs were taken of the jet at various velocities and ambient jet pressures. Before this could be done, it was necessary to find a means of cleaning the spray from the inside of the test-section walls; the method used consisted of causing a solid sheet of water to flow down this face for a brief interval of time which effectively wiped off the spray. The photograph was then quickly taken before sufficient spray had collected to cloud the walls and obscure the jet again. Figure 14 shows the typical result of these photographic studies, leaving no doubt as to the necessity for contact viewing windows if the interior of a free jet is to be viewed. Only at velocities below 10 fps did the jet surface become smooth, and at these low velocities the gravitational effect on the free jet is pronounced. The viewing windows subsequently employed in this setup have been described previously and are shown in Fig. 11.

The next step was the development of the cavitation head supporting system. The basic requirements were that the system should form adequate structural support; that the flow disturbances resulting from it be a minimum; that foreign material in the flow should not collect on the leading edge; and that it be capable of transmitting the pressure within steady-state cavitation bubbles formed about it. Type E of Fig. 12 represents the result of considerable experimental cut-and-try design. There were limiting factors such as the small scale involved, the high content of foreign material in the water, and the extremely low water temperatures (34° F) which necessitated such a procedure. The flow disturbance was minimized by using a single very slim and symmetrically streamlined strut which was sufficiently wide to give the required structural strength. The elimination of foreign material which tended to collect on the leading edge of the strut was accomplished by placing the strut at a small angle (30°) with the jet direction, resulting in an effective sweeping action on the leading edge.

The most difficult problem was that of accurately transmitting the bubble pressure. A fully developed steady-state cavitation bubble at low cavitation indices is almost entirely vapor filled so that the logical transmitting medium to use is this gaseous phase. This means that the pressure line must be free of water in order to insure accurate pressure transmission. The pressure line through the support system was kept clear of water while cavitation bubbles were in the process of formation by bleeding air in through this line. However, even after the steady-state cavity is formed the line may

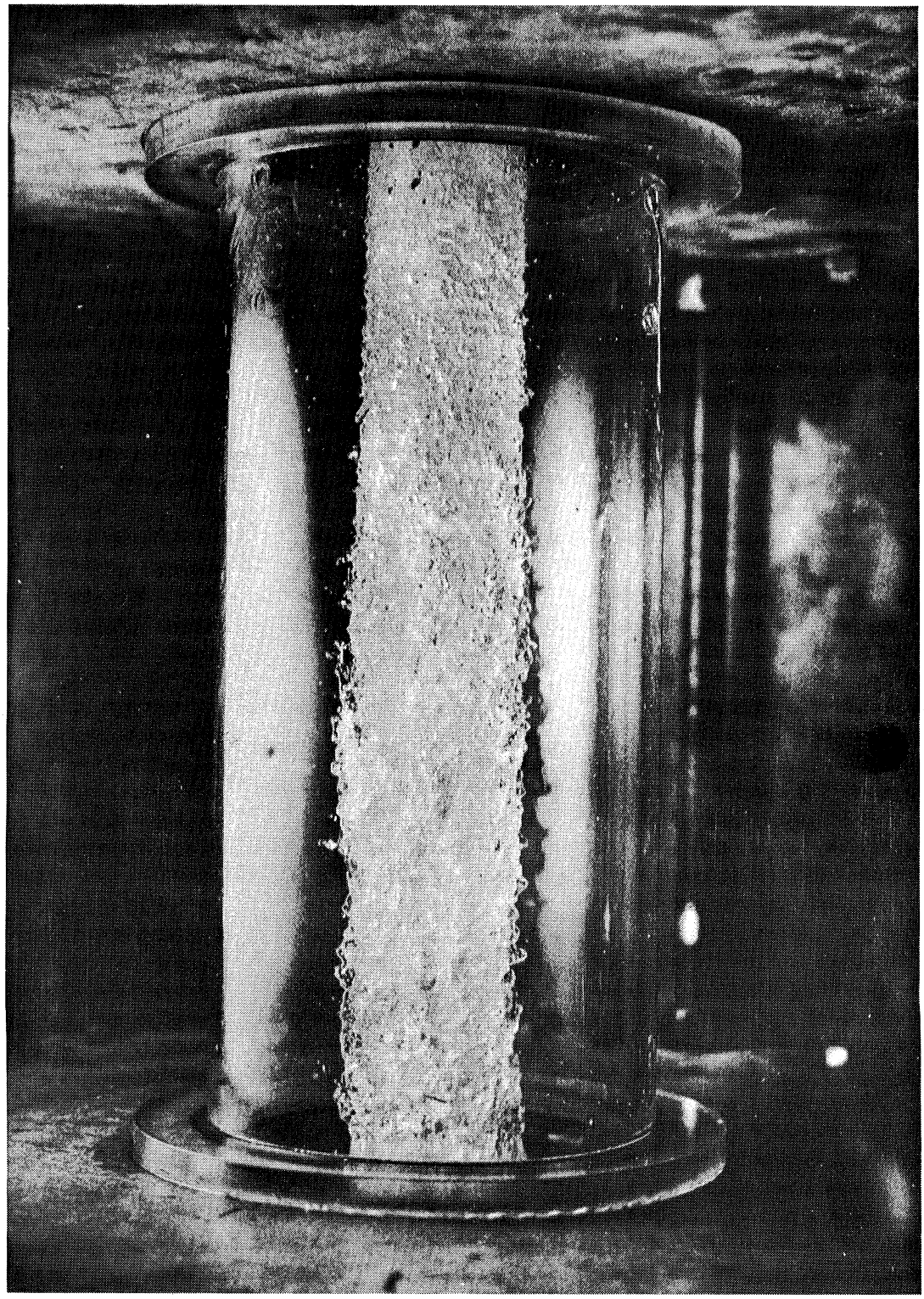

Fig.14— The 2-Inch Free Jet as Seen Through Test Section Without Viewing Windows. U = 40 fps (t = 10 microsec)

be plugged by water which condenses inside the bubble and which is discharged into the bubble by the reentrant jet which forms at the tail end of the bubble. For these reasons it became necessary to locate the piezometer taps on the rod in "ears" as shown on strut E so that the water which condensed on the rod ran around the taps rather than into them and to construct the conical block on the rod, also shown on type E, to protect the piezometer taps from the reentrant jet. Even with these precautions it was not possible to obtain pressure readings within steady-state cavitation bubbles described by cavitation indices greater than 0.05. These difficulties were greatly magnified, of course, by the extremely small scale at which the studies were carried on.

Figure 15 consists of three high-speed photographs showing the reentrant jet condition. The condition shown for $\sigma_k \simeq 0.045$ is an unsteady one in which the reentrant jet appears to oscillate, at times shooting as far forward as shown and at times consisting only of a foaming region where the bubble closes in the rear. The condition shown for $\sigma_k \simeq 0.08$ appears to be a steady one in which the reentrant jet consists entirely of this foaming region. Whether this latter condition is a true reentrant jet may be questionable. In the condition shown for $\sigma_k \simeq 0.025$, the reentrant jet is again limited to this foaming region except for occasional bursts of the jet into the interior of the bubble; however, the cavitation bubble is much larger and the presence of the reentrant jet is not critical for pressure measuring purposes.

After arriving at the final design for the cavitation head support system, a series of photographs was taken of cavitation bubbles for which the value of σ_k was accurately determined. In order to determine the distortion of these photographs due to photographing through the viewing windows and the jet, a grid was constructed, placed in the jet, and photographed also. From this a length-to-width distortion factor was determined as was the total width of the jet covered by the windows (3/4 in. or 37.5 per cent of the jet diameter). A series of these photographs is shown in Figs. 16 and 17, taken by a shadowgraph method which proved very useful. All of these latter photographs were taken at 1/50 sec, giving a smooth time-averaged bubble, and the cavitation head used had a base diameter of 3/16 in. and an included angel of 45°. The ratio of the maximum bubble diameter, d_m, to the axial bubble length, ℓ, was determined for purposes of comparison with similar data obtained with the jet horizontal. These values are plotted in Fig. 18 against σ_k as the independent variable.

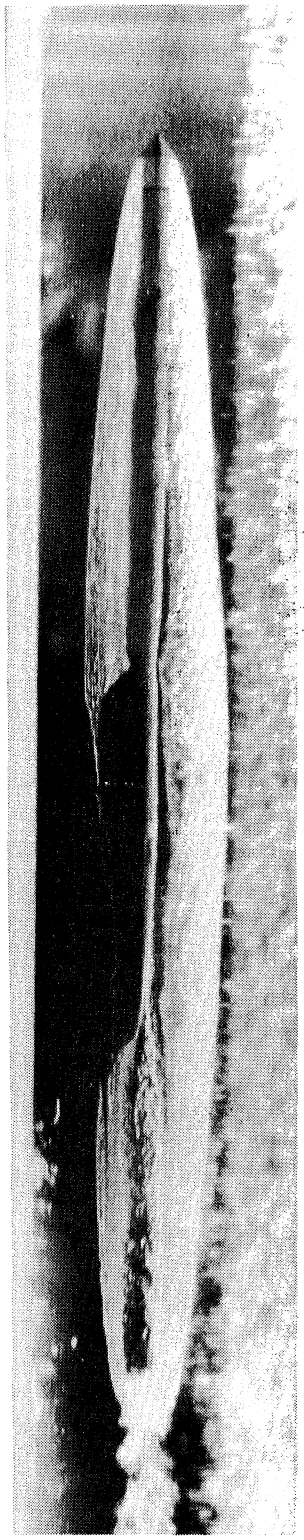

$\sigma_K \simeq 0.025$

$\sigma_K \simeq 0.045$

$\sigma_K \simeq 0.08$

Fig. 15 - Steady-State Cavitation Bubbles (t = 10 microsec)

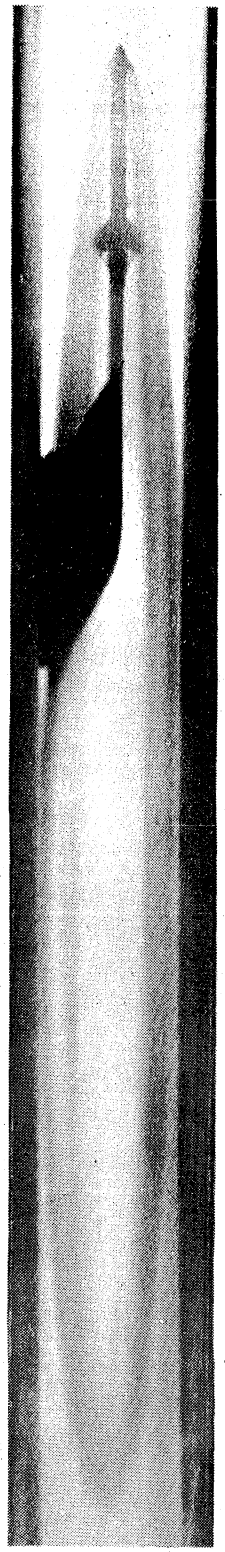

$\sigma_K = 0.014$

$\frac{dm}{\ell} = 0.083$

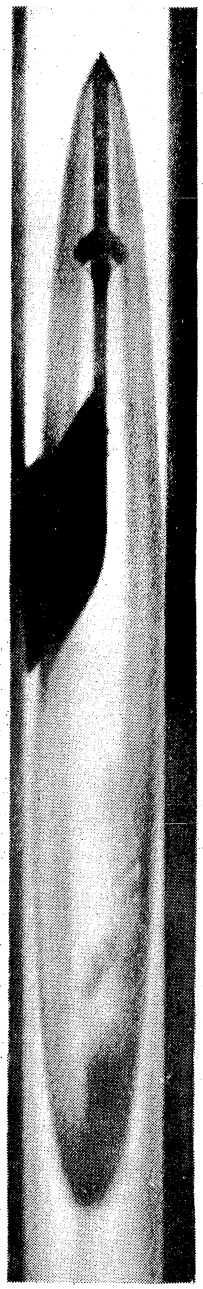

$\sigma_K = 0.018$

$\frac{dm}{\ell} = 0.093$

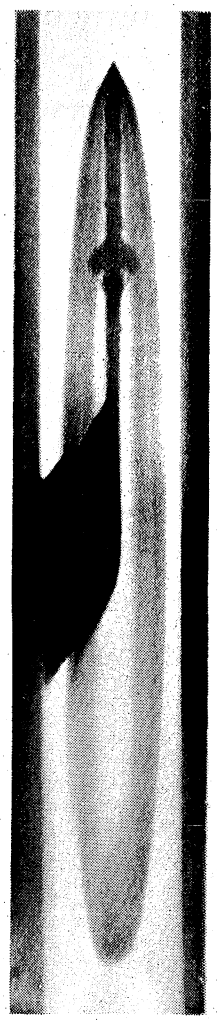

$\sigma_K = 0.021$

$\frac{dm}{\ell} = 0.097$

Fig. 16 — Steady-State Cavitation Bubbles ($t = \frac{1}{50}$ sec)

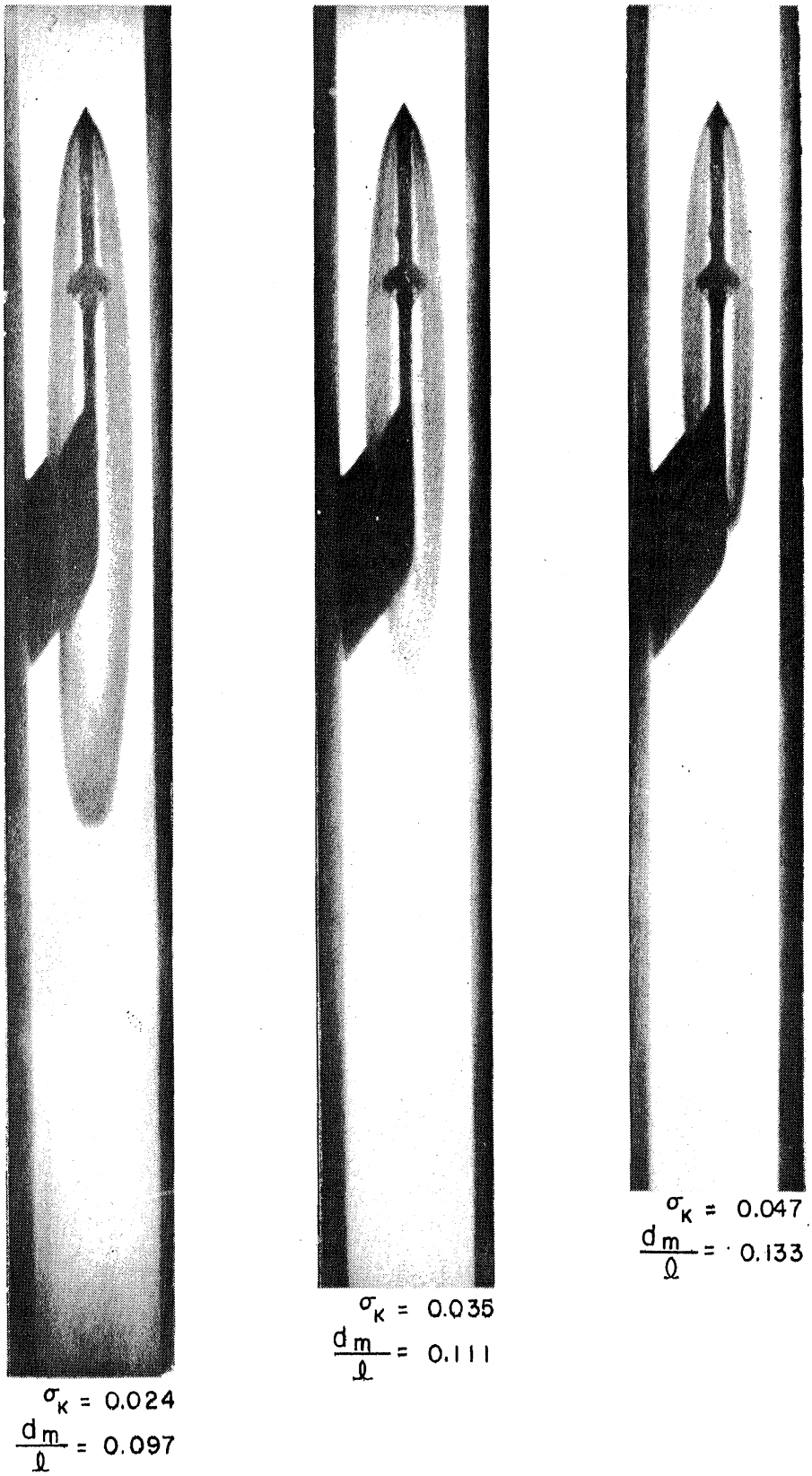

Fig. 17 – Steady-State Cavitation Bubbles ($t = \frac{1}{50}$ sec)

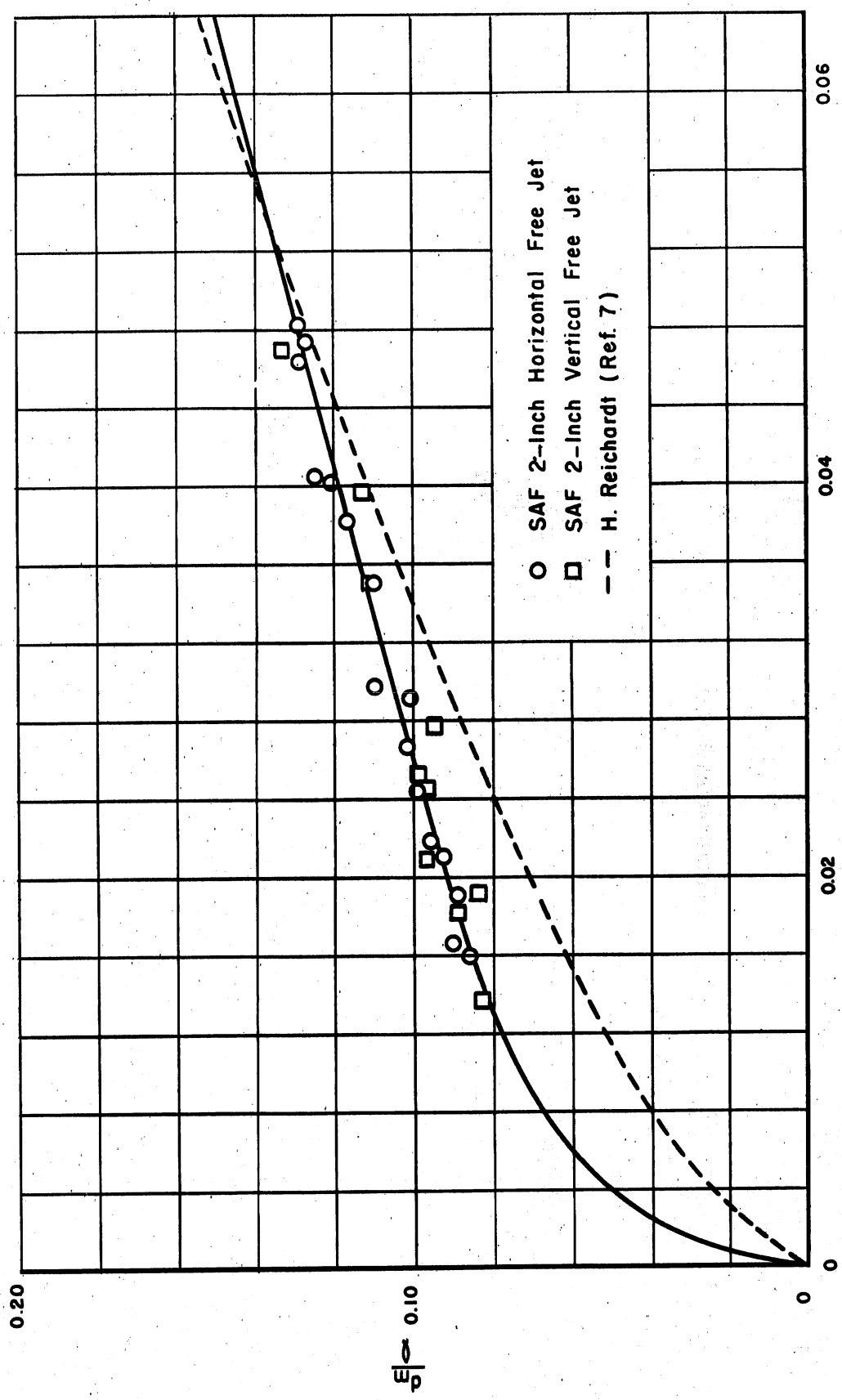

Fig. 18 — The Ratio $\frac{dm}{Q}$ of Steady-State Cavities as a Function of the Cavitation Index

As can be seen from Fig. 17, the largest cavitation bubbles photographed covered the entire width of the viewing region. This was not particularly critical, however, as when the bubble size was only slightly increased the bubble ruptured entirely. Hence it might be advantageous to increase the width of the viewing region to as high as 50 per cent of the jet diameter but any increase beyond this seems unwarranted. The method used for determining the ratio of d_m/Q should probably be noted. Again the small scale involved proved to be a limiting factor. The length of the bubble was determined by sketching in the undefined tail portion of the bubble on the photographic negatives so that it was symmetrical with the head end. The maximum width was also determined from the negatives. The ratio d_m/Q was then computed and corrected by the distortion factor mentioned above to give the true value of d_m/Q used in Fig. 18. Another means of defining the length of the bubble, which consisted of locating the point of maximum bubble diameter and taking twice the distance from this point to the front of the cavitation head as the length, was considered but was not used because of the difficulty of locating this point.

Total head traverses of the jet were made (using the Pitot tube and Pitot cylinder described previously) for the following boundary conditions: (1) no viewing windows in place, (2) one viewing window in place, and (3) two viewing windows in place. These traverses were made in two separate planes--one at a distance of 1.125 diameters downstream of the contraction exit and the other at a distance of 5.625 diameters downstream of the contraction exit. The jet velocity was 21.5 fps and the effective jet length was taken as 6 diameters or 12 inches. The Froude number based on the jet length was then 14.3. The traverses were taken on a diameter (two in each plane except when no windows were being used) such that one traverse ran along a centerline through the viewing windows and the second ran perpendicular to the first. Readings were taken at intervals of 0.05 in. near the boundary where the total head was rapidly changing and at intervals up to 0.20 in. near the jet center where it was relatively constant. The results are shown in Figs. 19, 20, and 21, in which the velocity head, $U^2/2g$, at any point divided by the velocity head, $U_c^2/2g$, at the jet centerline is plotted against the relative position of each point on a diameter. The static pressure is assumed constant throughout the jet and equal to the ambient test-section pressure which was atmospheric for all traverses. The Froude number for each profile is based on the mean jet velocity at the nozzle exit and the distance that the point of measurement

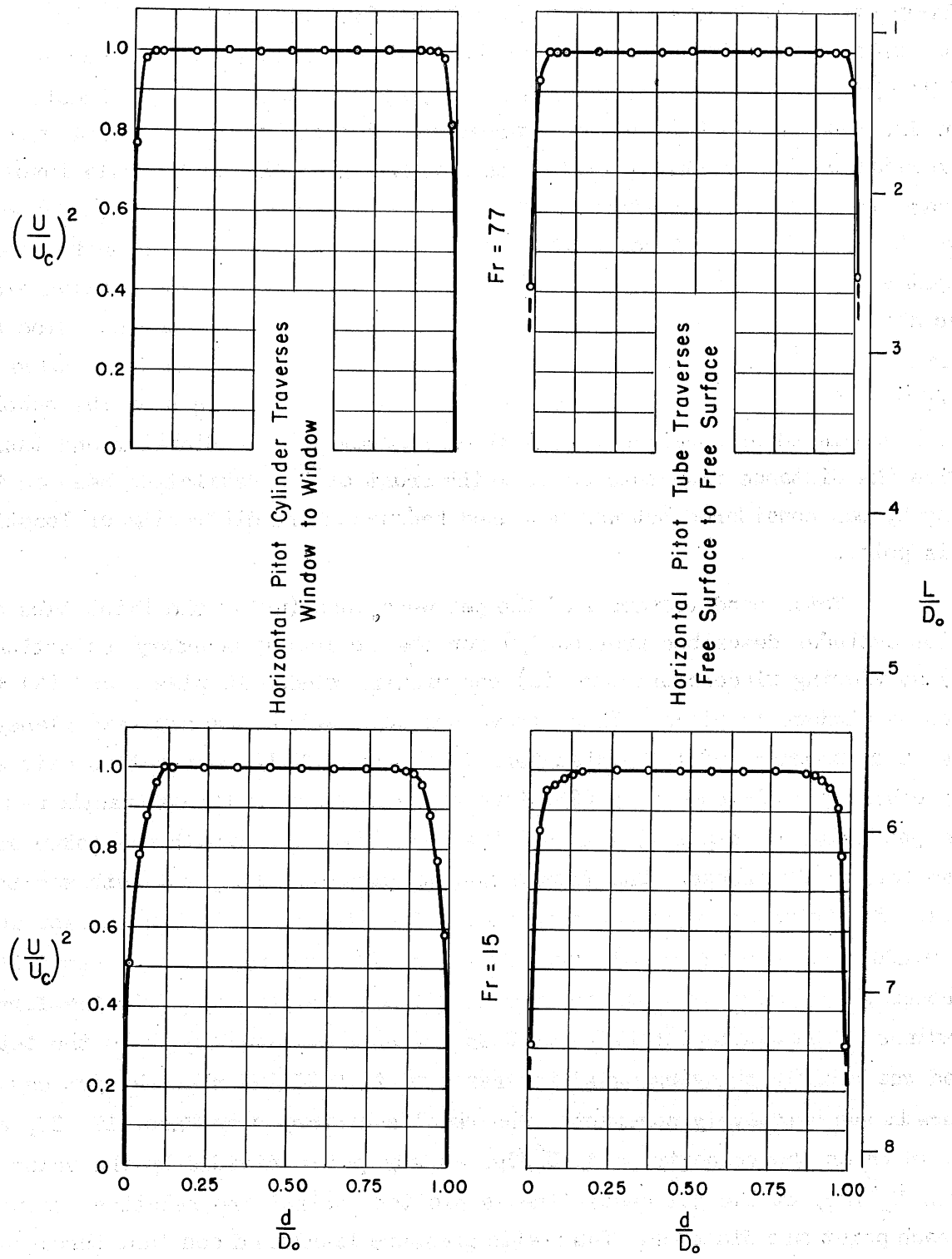

Fig. 19 – Velocity Head Traverses of a Vertical Jet
Two Viewing Windows in Place

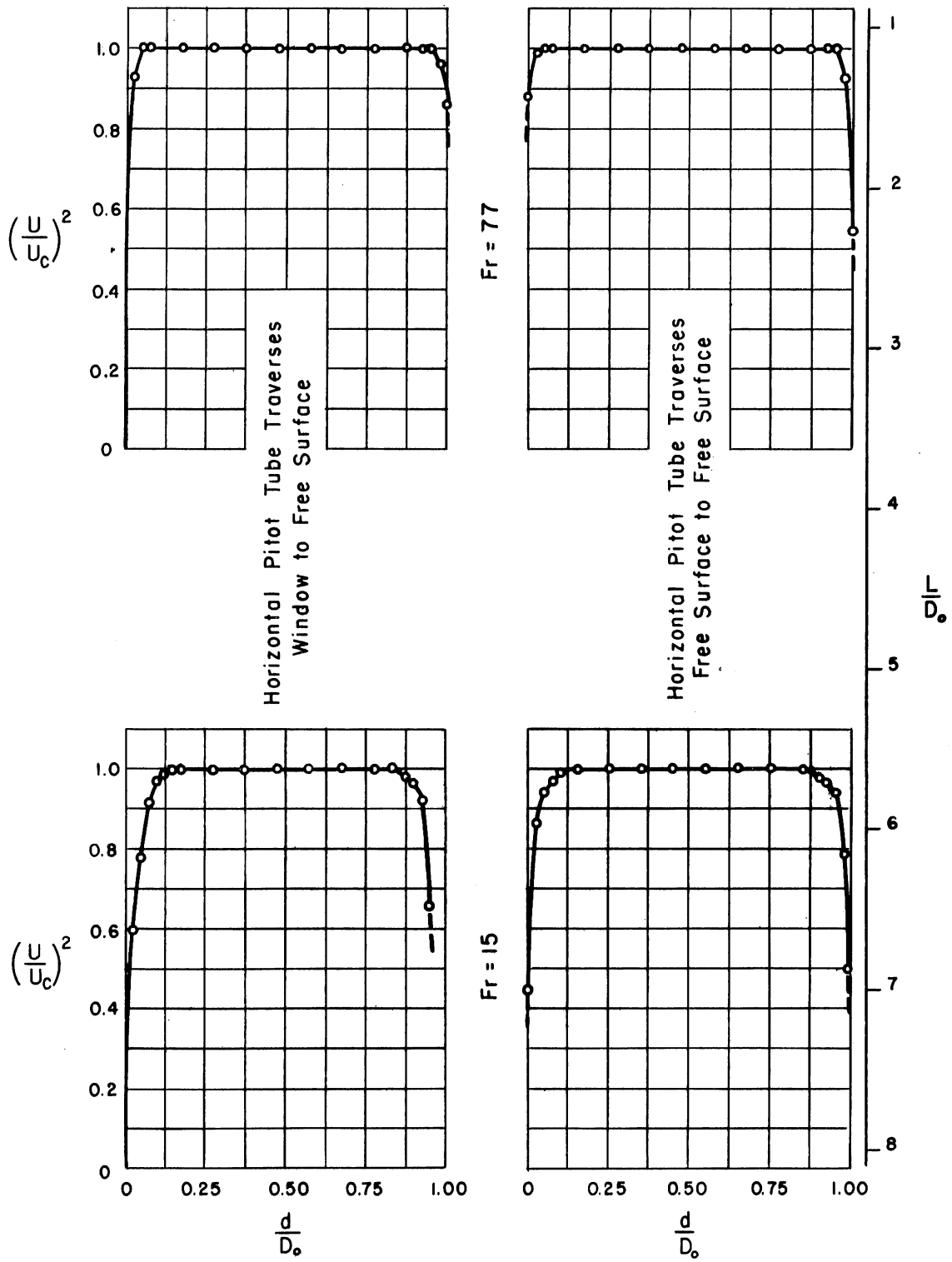

Fig. 20 – Velocity Head Traverses of a Vertical Jet
One Viewing Window in Place

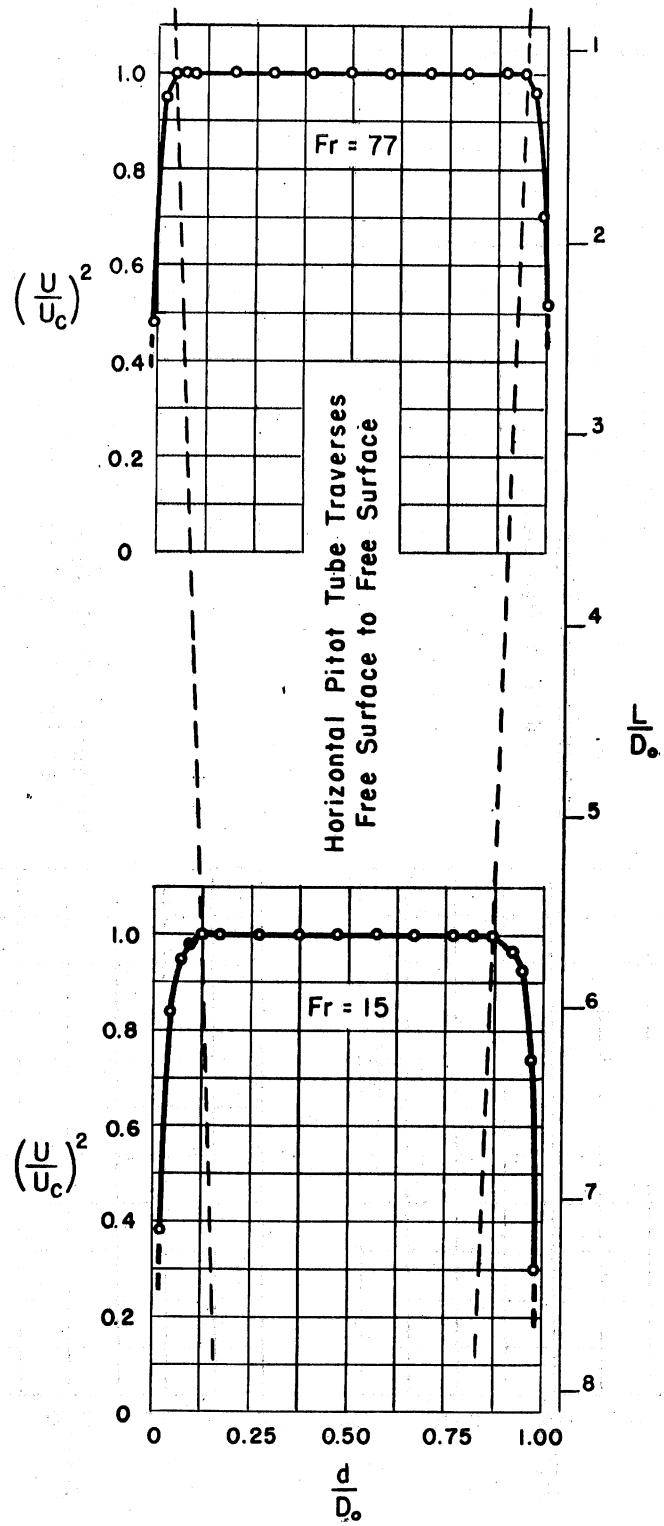

Fig. 21 – Velocity Head Traverses of a Vertical Jet
No Viewing Windows in Place

is located downstream of the nozzle exit. These figures indicate there is a drop in total head near the boundary irrespective of whether the boundary takes the form of a solid viewing window or a gaseous envelope, and the rate at which this boundary effect extends into the jet is approximately the same for the two cases. However, the drop in total head near the solid boundary is due to the formation of a boundary layer resulting from the viscosity of the flowing water, whereas the drop in total head near the free boundaries is an apparent drop in total head caused by the fact that the jet is entraining air through the surface of the jet. Each is just as detrimental as the other and it is gratifying that the rate at which they progress into the jet is of the same order of magnitude for both.

The dashed lines of Fig. 21 show the outline of the core flow when there are no viewing windows in place; hence these lines should indicate the depth to which the air entrained through the jet surface has progressed. According to this plot, the effective diameter of the jet 5 diameters downstream of the contraction exit is only 75 per cent of that at the contraction exit. This can be stated quantitatively only for this particular case, as the depth within the surface to which the entrained air penetrates in a given distance is a function of the flow velocity and turbulence; however, because of the unrefined design employed in this model tunnel, it should be on the side of safety to use this as a design factor since the turbulence level is probably quite high. An attempt was made to reduce the intensity of the jet turbulence by introducing screens in the approach pipe just upstream of the nozzle [14]. However, the foreign material in suspension in the river water being used quickly blocked these screens and led to the eventual abandonment of these particular tests without having achieved any useful results.

The last stage of the experimental studies was carried out with the jet directed horizontally as shown in Fig. 7. That portion of the water tunnel upstream of and including the test section was merely reoriented to form the horizontal free-jet water tunnel. However, that portion downstream of the test section was rebuilt entirely in order to prevent flooding of the test section. In order to achieve low test-section pressures in the horizontal free-jet water tunnel, it was necessary to connect it to the Laboratory's vacuum pumping system. The procedure followed was essentially that followed when the jet was directed vertically downward except that now all of the developmental work had been completed. Here it was only necessary to take a

series of photographs of steady-state cavities for comparison with those taken with the jet directed vertically downward and to take total head traverses of the jet. The ratio of d_m/ℓ for the horizontal cavitation bubbles was determined as described above for the vertical bubbles and these values were plotted on Fig. 18 against σ_k. It was thought that this plot might give a key to the type and the extent of the gravitational effect on the steady-state cavities in the free jet. However, as can be seen from Fig. 18, the scatter of the results for both the vertical and the horizontal free jet is such as to preclude drawing any conclusions from these studies concerning the gravitational effect. As a point of interest, the data and theory of H. Reichardt [7] are also shown in Fig. 18 as represented by the single dashed line. The discrepancy between this and the St. Anthony Falls data may be due to different methods of determining d_m/ℓ; and it may be due to the fact that the physical problem was not identical in the two cases, as Reichardt's measurements were made on artificial cavities, i.e., cavities formed by emitting a stream of air behind a body. It seems questionable, except under very carefully controlled test conditions, that a jet of air introduced behind a body would result in the same cavity outline as would result from natural cavitation.

The total head traverses of the horizontal free jet are shown in Figs. 22, 23, and 24. As can be seen, a total of twelve Pitot traverses were made of the horizontal jet--two at each station for the condition of no viewing windows in place, one viewing window in place, and two viewing windows in place. The stationing and the jet velocity were the same as for the vertical jet and the Froude number at each station was computed on the same basis as for the vertical jet also. The flow direction at the downstream station is at an angle of slightly less than 5° with the Pitot tube centerline for the vertical traverses, i.e., the traverses are taken perpendicular to the centerline of the contraction rather than perpendicular to the direction of the jet at either station. As a consequence, the measured value of the velocity head is slightly below the actual value; however, this variation should be nearly constant over a vertical traverse and therefore should not affect the dimensionless plot of U^2/U_c^2. Further, at the downstream station, the horizontal traverses are not through the centerline of the jet but through the extended centerline of the contraction which was approximately $0.2D_o$ above the former; however, the horizontal traverses indicate a constant total head and, under the assumption of constant static pressure equal to the ambient pressure, a

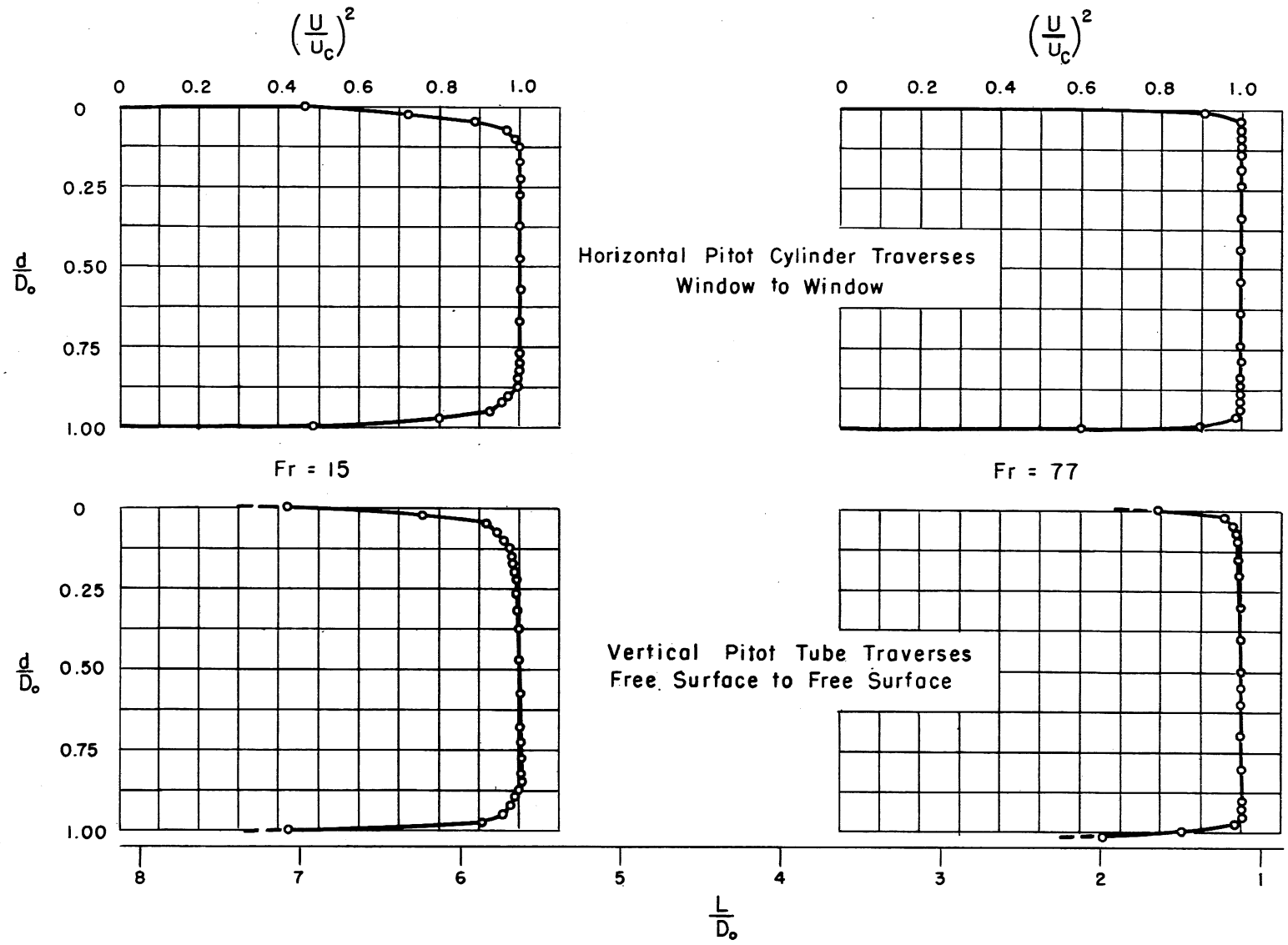

Fig. 22 - Velocity Head Traverses of a Horizontal Jet
Two Viewing Windows in Place

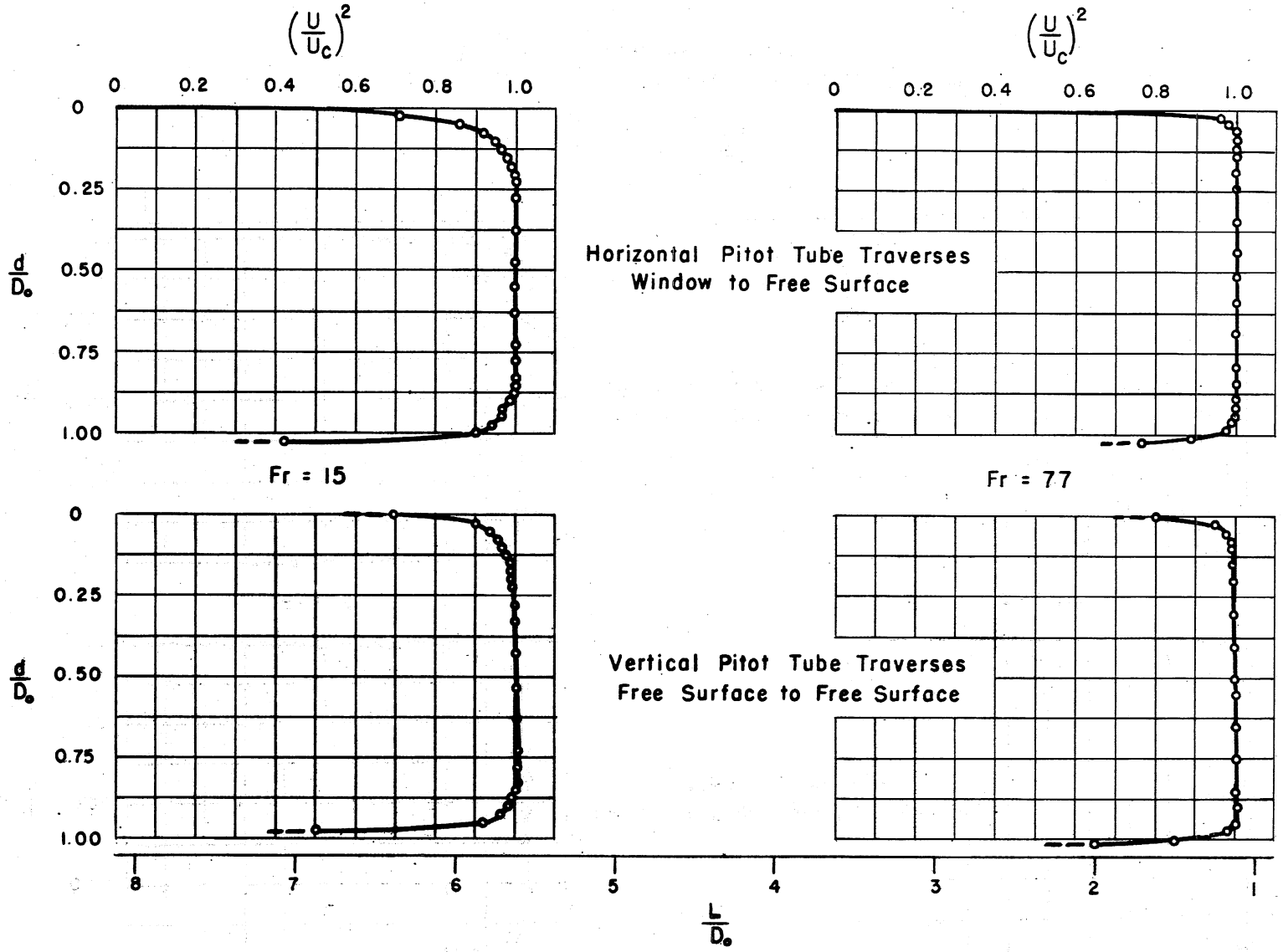

Fig. 23 - Velocity Head Traverses of a Horizontal Jet
One Viewing Window in Place

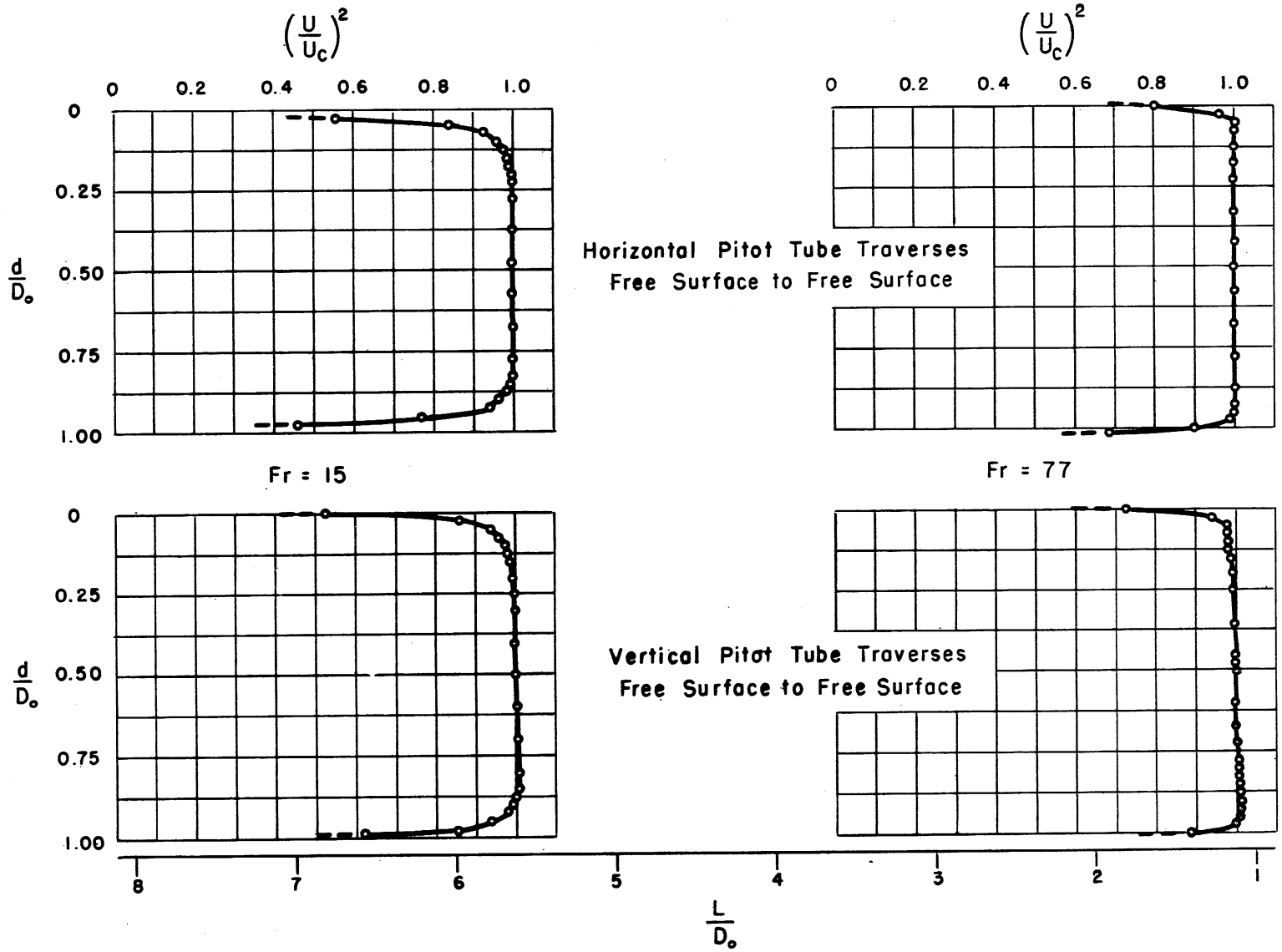

Fig.24 – Velocity Head Traverses of a Horizontal Jet
No Viewing Window in Place

constant velocity head from point to point on a horizontal line near the jet center. The vertical traverses, on the contrary, indicate an increasing total head from the top of the jet to the bottom of the jet, excepting the apparent boundary layer. The Froude number of the flow for these tests, based on the jet diameter, is $Fr_D = 86$ which indicates that as an approximation an increase in the velocity of the jet of 2.3 per cent should be expected in a vertical diameter, i.e., applying Bernoulli's equation at the top of the jet and at the bottom at the contraction exit. As can be seen, the measured traverses indicate a uniform variation of this order of magnitude.

V. SUMMARY

The following statements summarize, in so far as possible, the results and conclusions of this paper:

1. The free-jet water tunnel is a practical (and essential) device for implementing studies involving steady-state cavitation bubbles at low cavitation indices.

2. It is preferable that the energy of the jet in a free-jet water tunnel be allowable as an energy loss; however a part of this energy could be regained if the jet were directed vertically upward.

3. The flow through the test section should preferably be of a one-pass nature (i.e., non-recirculating) in order that: (a) the necessity for separating entrained air from the flow be eliminated, and (b) the rapid temperature rise of the water resulting from dissipation of the jet energy be eliminated. If this is not possible then consideration must be given to incorporating positive means for air separation into the tunnel design.

4. Viewing windows in contact with the jet are essential for viewing the interior of the jet.

5. No conclusion could be reached as to the effect of gravity on steady-state cavitation bubbles as evinced by changes in bubble configuration with changes in jet direction.

6. The jet of a free-jet water tunnel should preferably be directed vertically downward (unless the jet energy is to be regained) as this design results in: (a) minimum spray effects and natural drainage from the test section; (b) efficient natural aspiration of the air within the test section,

eliminating the necessity for employing a high vacuum pump to do this when the flow is non-recirculating; (c) minimum symmetrical gravitational effects which do not give rise to the pressure and velocity gradients which occur in the nonsymmetrical gravitational distortion of a horizontal free jet; and (d) an advantageous effect of gravity on the reentrant jet of the steady-state cavitation bubbles.

7. The free jet (with viewing windows in place) consists of a core flow of constant or nearly constant total head surrounded by a boundary layer composed of two parts: (a) the boundary layer opposite the viewing windows consists of a region of retarded flow due to viscous shear action between the jet and the windows; and (b) the boundary layer at the free surface consists of an apparent retarded flow due to air entrained into the flow through this surface. Both are of the same order of magnitude at any given distance downstream of the contraction and within a normal test-section length.

REFERENCES

[1] Reichardt, H. On Cavitation Tunnels for Small Cavitation Numbers. Kaiser Wilhelm Institute for Fluid Motion Research, Göttingen, Germany, February, 1945. Translated by N. Simmons, Issued by Royal Aircraft Establishment, London. November, 1945.

[2] Eisenberg, P. and Pond, H. L. Water Tunnel Investigations of Steady-State Cavities. U. S. Department of the Navy, David Taylor Model Basin Report No. 668. October, 1948.

[3] Allen, C. M. and Hooper, L. J. "Piezometer Investigations." Transactions, American Society of Mechanical Engineers, Vol. 54, Section Hyd 54-1, pp. 1-16. May, 1932.

[4] Simmons, N. The Geometry of Liquid Cavities with Especial Reference to the Effects of Finite Extent of the Stream. Ministry of Supply, Armaments Design Establishment, Technical Report No. 17/48. August, 1948.

[5] Birkhoff, G., Plesset, M., and Simmons, N. "Wall Effects in Cavity Flow." Quarterly of Applied Mathematics, Vol. 8, No. 2, pp. 151-68. July, 1950.

[6] Holdhusen, J. S. Model Studies for the Design of an Open- or Closed-Jet Water Tunnel. University of Minnesota, St. Anthony Falls Hydraulic Laboratory Project Report No. 22, June, 1950. 156 pages.

[7] Reichardt, H. The Laws of Cavitation Bubbles at Axially Symmetrical Bodies in a Flow. Ministry of Aircraft Production (Great Britain), Reports and Translations No. 766. August, 1946.

[8] Eisenberg, P. On the Mechanism and Prevention of Cavitation. U. S. Department of the Navy, David Taylor Model Basin Report No. 712. July, 1950.

[9] Rouse, H., Howe, J. W., and Metzler, D. E. Experimental Investigation of Fire Monitors and Nozzles. State University of Iowa, Iowa Institute of Hydraulic Research Report No. 3. November, 1949.

[10] Armstrong, A. H. and Hicks, E. P. The Distribution of Velocity and Pressure in an Open-Jet Cavitation Tunnel. Ministry of Supply (Great Britain), Armament Research Establishment Report No. 13/50. June, 1950.

[11] Gibson, A. H. Hydraulics and Its Applications (Fourth Edition). London: Constable and Company Ltd., p. 133 and p. 420, 1930.

[12] Holdhusen, J. S. and Ripken, J. F. Model Experiments for the Design of a Sixty-Inch Water Tunnel, Part II Contraction Studies. University of Minnesota, St. Anthony Falls Hydraulic Laboratory Project Report No. 11, September, 1948. 22 pages.

[13] Rosenberg, B. The Drag and Shape of Air Bubbles Moving in Liquids. U. S. Department of the Navy, David Taylor Model Basin Report No. 727. September, 1950.

[14] Schubauer, G. B., Spangenberg, W. G., and Klebanoff, P. S. Aerodynamic Characteristics of Damping Screen. National Advisory Committee for Aeronautics Technical Note No. 2001. January, 1950.

DISTRIBUTION LIST FOR PROJECT REPORT NO. 25
of the St. Anthony Falls Hydraulic Laboratory

Copies	Organization
6	Office of Naval Research, Department of the Navy, Washington 25, D. C., Attn: Mechanics Branch (Code 438).
1	Commanding Officer, Branch Office, U. S. Navy Office of Naval Research, 495 Summer Street, Boston 10, Massachusetts.
1	Commanding Officer, Branch Office, U. S. Navy Office of Naval Research, 346 Broadway, New York 13, N. Y.
2	Commanding Officer, Branch Office, U. S. Navy Office of Naval Research, 844 North Rush Street, Chicago 11, Illinois.
1	Commanding Officer, Branch Office, U. S. Navy Office of Naval Research, 801 Donahue Street, San Francisco 24, California.
1	Commanding Officer, Branch Office, U. S. Navy Office of Naval Research, 1030 East Green Street, Pasadena 1, California.
2	Officer in Charge, U. S. Navy Office of Naval Research, Branch Office, Navy 100, F.P.O. New York, N. Y.
9	Director, Naval Research Laboratory, Office of Naval Research, Washington 25, D. C., Attn: Technical Information Officer.
1	Executive Secretary, Research and Development Board, The Pentagon, Washington 25, D. C.
1	Chief of Naval Operations, Washington 25, D. C., Attn: DONO (Air).
1	Superintendent, U. S. Naval Postgraduate School, United States Naval Academy, Annapolis, Maryland.
1	Bureau of Aeronautics, Department of the Navy, Washington 25, D. C., Attn: Director, Airborne Equipment Division.
1	Bureau of Aeronautics, Department of the Navy, Washington 25, D. C., Attn: Design Elements Division.
1	Bureau of Ordnance, Department of the Navy, Washington 25, D. C., Attn: Code Ad3.
1	Naval Ordnance Laboratory, White Oak, Silver Spring 19, Maryland, Attn: Mechanics Division.
1	Underwater Ordnance Department, U. S. Naval Ordnance Test Station, Pasadena Annex, 3202 East Foothill Boulevard, Pasadena 8, California.
1	Naval Torpedo Station, Newport, Rhode Island.

Copies	Organization
1	Bureau of Ships, Department of the Navy, Washington 25, D. C., Attn: Research Division.
1	Bureau of Ships, Department of the Navy, Washington 25, D. C., Attn: Propeller and Shafting Branch.
6	David Taylor Model Basin, Washington 7, D. C., Attn: Hydromechanics Department.
1	Bureau of Yards and Docks, Department of the Navy, Washington 25, D. C., Attn: Research Division.
1	Underwater Sound Laboratory, Fort Trumbull, New London, Connecticut.
1	Waterways Experiment Station, Vicksburg, Mississippi.
1	Office of the Chief of Engineers, Gravelly Point, Virginia, Attn: Engineering Division.
1	Air Materiel Command, Wright-Patterson Air Force Base, Dayton, Ohio, Attn: Air Documents Division.
1	Director of Research, National Advisory Committee for Aeronautics, 1724 F Street, N. W., Washington 25, D. C.
1	Geological Survey, Department of the Interior, Washington 25, D. C., Attn: C. G. Paulsen, Chief Hydraulic Engineer.
1	Bureau of Reclamation, Denver, Colorado, Attn: I. A. Winter.
1	National Bureau of Standards, National Hydraulic Laboratory, Washington 25, D. C., Attn: H. N. Eaton.
1	Captain H. E. Saunders, 206 Maple Avenue, Takoma Park, Washington 12, D. C.
1	Columbia University, Department of Civil Engineering, New York 27, N. Y.
1	Illinois Institute of Technology, Department of Fundamental Mechanics Research, Chicago 16, Illinois, Attn: Dr. V. L. Streeter.
1	The Johns Hopkins University, Mechanical Engineering Department, Baltimore, Maryland, Attn: Dr. G. F. Wislicenus.
1	Massachusetts Institute of Technology, Department of Civil and Sanitary Engineering, Cambridge 39, Massachusetts, Attn: Dr. A. T. Ippen.
1	Massachusetts Institute of Technology, Department of Naval Architecture and Marine Engineering, Cambridge 39, Massachusetts, Attn: Admiral E. L. Cochrane.

Copies	Organization
1	University of Michigan, Engineering Mechanics Department, Ann Arbor, Michigan, Attn: Prof. R. A. Dodge.
1	University of Minnesota, St. Anthony Falls Hydraulic Laboratory, Minneapolis 14, Minnesota, Attn: Dr. L. G. Straub.
1	Northwestern University, Department of Civil Engineering, Evanston, Illinois, Attn: Prof. W. S. Hamilton.
1	University of Notre Dame, College of Engineering, Notre Dame, Indiana, Attn: Dean K. E. Schoenherr.
1	The Pennsylvania State College, School of Engineering, Ordnance Research Laboratory, State College, Pennsylvania.
1	University of Southern California, Department of Physics, Los Angeles, California, Attn: Dr. R. E. Vollrath.
1	Stanford University, Department of Civil Engineering, Stanford, California, Attn: Prof. J. K. Vennard.
1	University of Tennessee, Engineering Experiment Station, Knoxville, Tennessee, Attn: Dr. G. H. Hickox.
1	Woods Hole Oceanographic Institute, Woods Hole, Massachusetts, Attn: Dr. Columbus Iselin.
1	Worcester Polytechnic Institute, Alden Hydraulic Laboratory, Worcester, Massachusetts, Attn: Prof. L. J. Hooper.
1	Kimberly Clark Corporation, Research and Development Laboratories, Neenah, Wisconsin, Attn: C. A. Lee.
1	Library, California Institute of Technology, Pasadena 4, California.
1	Engineering Societies Library, 29 West 39th Street, New York, N. Y.
1	John Crerar Library, Chicago 1, Illinois.
1	Library, Massachusetts Institute of Technology, Cambridge 39, Massachusetts.
1	Polytechnic Institute of Brooklyn, 99 Livingston Street, Brooklyn 2, New York, Attn: Dr. L. Meyerhoff.
1	Library, University of Texas, Austin, Texas.
1	Dr. E. Cooper, Chairman, Underwater Ordnance Department, Naval Ordnance Test Station, 3202 East Foothill Boulevard, Pasadena 8, California.

Copies	Organization
1	Prof. G. Birkhoff, Department of Mathematics, Harvard University, 21 Vanserg Building, Cambridge 38, Massachusetts.
1	Dr. F. H. Clauser, Department of Aeronautics, The Johns Hopkins University, Baltimore 18, Maryland.
1	Dr. J. W. Daily, Department of Civil and Sanitary Engineering, Massachusetts Institute of Technology, Cambridge 39, Massachusetts.
1	Dr. K. S. M. Davidson, Experimental Towing Tank, Stevens Institute of Technology, 711 Hudson Street, Hoboken, New Jersey.
1	P. Eisenberg, Hydromechanics Department, David Taylor Model Basin, Washington 7, D. C.
1	Dr. R. T. Knapp, Hydrodynamics Laboratories, California Institute of Technology, 1201 East California Street, Pasasena 4, California.
1	Dr. F. A. Maxfield, Bureau of Ordnance (Code Re6a), Department of the Navy, Washington 25, D. C.
1	Dr. J. H. McMillen, Naval Ordnance Laboratory, White Oak, Silver Spring 19, Maryland.
1	Dr. A. Miller, Bureau of Ordnance (Code Re3d), Department of the Navy, Washington 25, D. C.
1	Dr. J. M. Robertson, Ordnance Research Laboratory, The Pennsylvania State College, State College, Pennsylvania.
1	Dr. H. Rouse, Iowa Institute of Hydraulic Research, State University of Iowa, Iowa City, Iowa.
1	Dr. J. H. Wayland, Department of Applied Mechanics, California Institute of Technology, 1201 East California Street, Pasadena 4, California.
3	Serials Division, Library, University of Minnesota, Minneapolis 14, Minnesota.

(Reference: ONR ltr. ONR:438:EH, NR-062-065 of October 31, 1950, to Director, St. Anthony Falls Hydraulic Laboratory.)